LONG CHAIN FATTY ACYL-COENZYME A SYNTHETASES AS NOVEL DRUG TARGETS IN *CRYPTOSPORIDIUM PARVUM*

A Dissertation

by

FENGGUANG GUO

Submitted to the Office of Graduate and Professional Studies of
Texas A&M University
in partial fulfillment of the requirements for the degree of

DOCTOR OF PHILOSOPHY

Chair of Committee,	Guan Zhu
Committee Members,	Jane Welsh
	Yanan Tian
	Sanjay Reddy
Head of Department,	Linda Logan

August 2014

Major Subject: Veterinary Microbiology

ABSTRACT

Cryptosporidium parvum infects both humans and animals, and continues to be a significant opportunistic pathogen among AIDS patients and one of the leading diarrheal pathogens in children. Despite decades of research on cryptosporidiosis including screening hundreds of compounds in vitro and in vivo, fully effective therapeutic agents are still unavailable. The major goal of this study is to explore three long-chain fatty acyl-CoA synthetase (CpACSs) of the parasite as novel drug targets. The molecular and biological data showed that the three CpACSs genes are differently expressed in the parasite different life cycle stages and their proteins display different subcellular distribution patterns in the parasite, suggesting that the those genes may play different biological roles in the parasite. Using recombinant proteins, we have determined detailed enzyme kinetics for CpACS1 and CpACS2, and observed that the inhibitor triacsin C could inhibit their enzyme activities with K_i in the nanomolar range. Triacsin C also effectively inhibited the growth of *C. parvum* parasites in vitro (IC_{50} = 136 nM). Most importantly, triacsin C effectively reduced parasite oocyst production up to 88.1% with no apparent toxicity when administered to *Cryptosporidium*-infected IL-12 knock-out mice at 15 mg/kg/d for one week. These observations not only validate CpACSs as a pharmacological target, but also indicate that triacsin C and analogs may be explored as potential new therapeutics against cryptosporidiosis.

DEDICATION

To Dr. Yuxi Duan, who opened the first door for me to start my scientific career, and he is always willing to help me whenever I need it.

To my parents, Yongxue and Guirong, who always support, encourage and love me through my life.

ACKNOWLEDGEMENTS

.

I would like express the deepest appreciation to my committee chair, Dr. Guan Zhu, for great guidance and support throughout the course of this research. He is always available, whenever I need him. I really appreciate his encouragement and friendship. Without his supervision and persistent help this dissertation would not have been possible. I sincerely thank my committee members, Dr. Jane Welsh, Dr. Yanan Tian, and Dr. Sanjay Reddy, for their invaluable advice and support during my graduate career.

Thanks go to our collaborators, Dr. Jan R Mead and Nina N. McNair, at Emory University, for in vivo drug assay.

Thanks also go to the past and present members in Dr. Zhu Laboratory: Dr. Haili Zhang, Dr. Xiangyu Shi, Dr. Mayte Yichoy, Dr. Lixin Xiang, Dr. Mingfei Sun, Dr. Yamei Jin, Dr. Jason M. Fritzler, Dr. S. Dean Rider, Lacy Parson, Mary Yu, and Rana Eltahan, for their friendly help. I would also like to thank my graduate advisor, Dr. Patricia Holman, graduate program coordinators, Stevie Bundy and Katie Cosby, for their kind helps. Thanks also go to my friends and colleagues and the department faculty and staff for making my time at the Texas A&M University a great experience.

I also want to thank my parents and parents-in-law, for their support and helping taking care of my children. Thanks go to my daughter, Lucy, and my son, Lucas. They are filling my life with rainbow colors.

A special thank goes to my wife. She has always stood by me, inspired me and provided constant encouragement during the entire process.

NOMENCLATURE

ABC	ATP-Binding Cassette
ACBP	Acyl-CoA Binding Protein
ACL	Acyl-CoA Ligase
ACP	Acyl Carrier Protein
ACS	Acyl-CoA Synthetase
AIDS	Acquired Immune Deficiency Syndrome
AL	Acyl-[Acyl Carrier Protein] Ligase
AMP	Adenosine Monophosphate
AT	Acyl-Transferase
ATP	Adenosine Triphosphate
BI	Bayesian Inference
BLAST	Basic Local Alignment and Search Tool
BSA	Bovine Serum Albumin
CD4	Cluster of Differentiation 4
CD8	Cluster of Differentiation 8
CDC	Centers for Disease Control and Prevention
CDS	Coding Sequence
CoA	Coenzyme A
COWP	*Cryptosporidium* Oocyst Wall Protein
CTP	Cytidine Triphosphate

DAPI	*4',6'*-Diamidino-2-Phenyl Indole
DIC	Differential Interference Contrast
DMSO	Dimethyl Sulfoxide
DNA	Deoxyribonucleic Acid
DTNB	5,5'-Dithio-Bis-(2-Nitrobenzoate)
DTT	Dithiothreitol
EDTA	Ethylenediaminetetraacetic Acid
ER	Enoyl-ACP Reductase
FAS	Fatty Acid Synthase
FBS	Fetal Bovine Serum
FDA	Food and Drug Administration
FITC	Fluorescein Iso-Thiocyanate
gDNA	Genomic Deoxyribonucleic Acid
GTP	Guanosine Triphosphate
HAART	Highly-Active Anti-Retroviral Therapy
HCT-8	Human Colonic Tumor 8
HIV	Human Immunodeficiency Virus
ICZN	Code of Zoological Nomenclature
IFN-γ	Interferon Gamma
IL-12	Interleukin 12
IPTG	Isopropyl-1-Thio-β-D Galactopyranoside
IgY	Immunoglobulin Y

LC	Long Chain
KS	Ketoacyl-CoA Synthase
KR	Ketoacyl-ACP Reductase
MBP	Maltose Binding Protein
MHC	Major Histocompatibility Complex
ML	Maximum Likelihood
MTT	Methylthiazol Tetrazolium
NCBI	National Center for Biotechnology Information
NIH	National Institutes of Health
NTP	Nucleoside Triphosphates
NTZ	Nitazoxanide
ORF	Open Reading Frame
PAGE	Polyacrylamide Gel Electrophoresis
PBS	Phosphate Buffered Saline
PCR	Polymerase Chain Reaction
PDB	Protein Database
PEG	Polyethylene Glycol
PKS	Polyketide Synthase
PI	Post-Infection
PP	Posterior Probability
PV	Parasitophorous Vacuole
PVM	Parasitophorous Vacuolar Membrane

qRT-PCR	Quantitative Reverse Transcriptase-Polymerase Chain Reaction
RNA	Ribonucleic Acid
rRNA	Ribosomal Ribonucleic Acid
RT-PCR	Reverse Transcriptase Polymerase Chain Reaction
SCID	Severe Combined Immune Deficient
SDS	Sodium Dodecyl Sulfate
SPF	Specific Pathogen-Free
TAMU	Texas A&M University
TBST	Tris Buffered Saline containing Tween 20
TDC	Taurodeoxycholic Acid
TRITC	Tetramethyl Rhodamine Iso-Thiocyanate
UTP	Uridine Triphosphate
VLC	Very Long Chain
WHO	World Health Organization

TABLE OF CONTENTS

Page

Page

LIST OF FIGURES

Page

LIST OF TABLES

Page

1 INTRODUCTION AND LITERATURE REVIEW

1.1 The history of *Cryptosporidium* spp.

Cryptosporidium was first observed in gastric glands of laboratory mice by Ernest Edward Tyzzer in 1907 (1). He precisely described its morphology and life cycle. The morphology of this protozoan parasite is similar to the coccidia, but lacking sporocysts, so that Tyzzer named it as *Cryptosporidium muris*. In 1912, the second species of *Cryptosporidium* was described in intestine of mouse by Tyzzer, and was named as *C. parvum* (2). For almost 70 years after the discovery, *Cryptosporidium* was regarded as an insignificant pathogen that infected the intestines of vertebrates and caused little or no disease. In 1976, the first human cryptosporidiosis was reported as an acute, self-limiting illness in an immunocompetent 3-year old child (3). In the same year, another human case was reported in an immnunocompromised patient (4). Since then, *Cryptosporidium* started to be recognized as a significant human pathogen. Among the first seven cases of human cryptosporidiosis reported between 1976 and 1980, six patients were immunosuppressed or immunocompromised, which led to the consideration of *Cryptosporidium* as an opportunistic pathogen (5). From 1976 to 1984, the reported cases of human cryptosporidiosis reached to 58, including 18 from immunocompetent individuals (6). Therefore, *Cryptosporidium* was recognized as a significant parasitic pathogen that is capable of infecting both immunocompromised and immnunocompetent patients. Cryptosporidial infections might result in severe and

chronic diarrhea in immunocompromised patients, or mild to severe symptoms but usually self-limiting in immunocompetent individuals.

In the late 1970s and early 1980s, several notable water-borne outbreaks of cryptosporidiosis brought more attentions from the government and public on this parasite. In 1978, an outbreak of cryptosporidiosis occurred in Carrollton, Georgia, United States of America (USA), due to the contamination of a filtered public water supply, affected about 13,000 people (7). Two years later, another outbreak in Wiltshire and Oxfordshire, UK affected around 5,000 people with 516 diagnosed cases. The most massive waterborne outbreak occurred in Milwaukee, Wisconsin, USA in 1993, in which estimated 403,000 people had watery diarrhea, and 4,400 people were hospitalized. The total costs associated with this outbreak were estimated at $96.2 million (8,9). Because of the potential of large-scale dissemination with moderate illness, and the requirement of specific enhancements of diagnostic capacity and disease surveillance, *Cryptosporidium* is listed as a category B priority agent in the Biodefense program by the National Institutes of Health (NIH) and the Centers for Disease Control and Prevention (CDC) in the USA (10). The significance in the public health and the potential of waterborne outbreaks motivated a substantial research effort to better understand the parasites. In the past two decades, studies have greatly expanded our knowledge of *Cryptosporidium* parasites, including taxonomy, epidemiology, transmission, host-parasite interaction and molecular biology. One of the milestones in the research during this period was the publication of the complete genome sequences of *C. parvum* (Iowa stain) and *C. hominis* (isolate TU502 isolate), which uncovered their

unique biological features characterized by the extremely streamlined metabolic pathways and a reliance on the host for nutrients (11,12). Although we have gained tremendous knowledge of those parasites from substantial studies, cryptosporidial waterborne outbreaks still occur yearly, and fully effective treatments are yet unavailable for this disease.

1.2 Taxonomy

The genus of *Cryptosporidium* belongs to the Phylum Apicomplexa, in which all members possess an apical complex at some stages in their life cycles. Within the Apicomplexa, *Cryptosporidium* is placed under the Class Conoidasida. However, the taxonomic relationship of *Cryptosporidium* under the Class has been under debate since last decade (13,14). Traditionally, *Cryptosporidium* has been considered as an intestinal coccidian because this genus of parasites share similar life cycle development and morphology with other coccidian species (15). However, increasing molecular and phylogenetic evidences support the fundamental biological differences between *Cryptosporidium* and the Coccidia, which include: (I) the location of *Cryptosporidium* in the host cell is intracellular, but extracytoplasmic; (II) the presence of thick-walled and thin-walled oocysts, rather than only thick-walled oocysts (16); (III) the small size of oocyst and lack of sporocyst (17); (IV) the lack of apicoplast and its genome (18); and (V) the insensitivity to most anticoccidial drugs (19). Recently, molecular phylogenic data indicates that *Cryptosporidium* is an early evolution branch at the base of the Apicomplexa, rather than as a sister to the other intestinal and cyst-forming coccidia

(14,20,21). Furthermore, phylogenic data of small-subunit rRNA and other genes or proteins suggest that *Cryptosporidium* is more closely related to the gregarines than to the coccidia (22). Additionally, the chloroplast-derived apicoplast is present in the three major apicomplexan lineages haemospororida, piroplasms and coccidia, but not in cryptosporidia and gregarines, suggesting that gregarines and *Cryptosporidium* might have a common ancestor, and apicoplast was lost following the divergence of gregarines and *Cryptosporidium* from other apicompelxans (23,24). A recent genome sequence survey (GSS) for *Ascogregerina taiwanensis* also supports the evolutionary affinity between a gregarine and *Cryptosporidium* (21). However, gregarines possess many metabolic pathways that are absent in *Cryptosporidium,* such as those for de novo synthesizing amino acids, pyrimidines, and purines (11,21).

Currently, there are 25 valid *Cryptosporidium* species (Table 1.1). In the earlier time, mainly oocyst morphology, hosts and infection sites characterized the species of *Cryptosporidium*. Ernest Edward Tyzzer described the first two species, *C. muris* and *C. parvum*, which were found in mouse gastric glands and small intestines, respectively (1,2,17). Those two species are still valid today. However, no new species was reported over half century, except that some species in the genus of *Sarcocystis* were erroneously assigned as new *Cryptosporidium* species (25). The errors were corrected after a unique attachment organelle was confirmed as one of the key features to define the *Cryptosporidium* genus in 1960s (25,26). Following this correction, another misleading feature, host specificity, was adopted from the coccidian classification system. Based on the host origin, multiple new *Cryptosporidium* species were mistakenly named. Until

early 1980s, cross-transmission experiments demonstrated that *Cryptosporidium* isolates could transmit across different host species, which ended the mistakes and many newly named species were merged to *C. parvum* (27-29). Due to lack of effective criteria to differentiate *Cryptosporidium* species, Levine in 1984 considered that only four species other than *C. parvum* were valid, including *C. muris* in mammals, *C. meleagridis* in birds, *C. crotali* in reptiles, and *C. nasorium* in fish (30).

After the *Cryptosporidium* was recognized as a significant human pathogen, how to differentiate the species of *Cryptosporidium* became necessary and critical to the understanding of parasite transmission and epidemiology (25,31). Because a single criterion was insufficient to different *Cryptosporidium* spp., the combination of several criteria was adapted. The genetic markers have been widely applied in defining new *Cryptosporidium* spp., particularly those derived from genes encoding 18S ribosomal RNA (rRNA), the hyper-variable 60-kDa glycoprotein (gp60), and the oocyst wall protein (COWP) (32,33). Through decades of studies, most researchers have accepted a relative stable and practical standard for *Cryptosporidium* speciation, which include: (I) oocyst morphology; (II) genetic characterization; (III) demonstration of natural and, whenever feasible, experimentally defined host specificity; (IV) compliance with International Code of Zoological Nomenclature (ICZN) (25,31,33). Based on the morphological, biological, and molecular data, 25 species of *Cryptosporidium* have been formally described and accepted as valid species (33).Those 25 species include one in fish, *C. molnari* (Alvarez-Pellitero and Sitja-Bobadilla 2002); one in amphibians, *C. fragile* (Jirku M et al. 2008); two in reptiles, *C. serpentis* (Levine1980) and

Table 1.1 The 25 currently confirmed Cryptosporidium species *

Cryptosporidium species	Major host(s)	Site(s) of infection	Oocyst size L x W(μm)	Reference	GenBank ID (18S rRNA)
C. molnari	Gilthead sea bream	Stomach and intestine	4.7 x 4.5	Alvarez-Pellitero & Sitja-Bobadilla 2002 (34)	HM243548 HM243550 HQ585890
C. fragile	Black-spined toads	Stomach	6.2 x 5.5	Jirku M et al.2008(35)	EU162751-EU162754
C. serpentis	Amazon tree boa	Stomach	6.2 x 5.3	Levine1980 (36)	AF151376
C. varanii	African fat-tailed geco	Intestine, cloaca	4.7 x 5.0	Pavlasek et al. 1995 (37)	AF112573
*C. meleagridis***	Turkey	Intestine	4.3 x 4.9	Slavin 1955 (38)	AF112574
C. baileyi	Chicken	Cloaca, bursa, trachea	6.4 x 4.8	Current et al. 1986 (39)	L19068
C. galli	Chicken	Preventriculus	8.3 x 6.3	Pavlasek 1999 (33)	AF316624, AY18847
C. muris	Rodents	Stomach	8.4 x 6.1	Tyzzer 1907 (1)	AB89284
C. parvum	Cattle, sheep, human	Small intestine	4.4 x 4.9	Tyzzer 1912 (2)	AF308600
C. wrairi	Guinea pigs	Small intestine	4.6 x 5.4	Vetterling et al. 1971 (40)	AF115378
*C. felis***	Cats	Small intestine	4.5 x 5.0	Iseki 1979 (41)	AF108862
C. andersoni	Cattle	Abomasum	5.5 x 7.4	Lindsay et al. 2000 (42)	AF093496
*C. canis***	Dogs	Small intestine	4.8 x 5.0	Fayer et al. 2001 (43)	AF112576
C. hominis	Humans	Small intestine	4.8 x 5.2	Morgan-Ryan et al. 2002 (44)	AF108865
C. suis	Pigs	Intestine	4.2 x 4.6	Ryan et al 2004 (45)	AF115377
C. bovis	Cattle	Small intestine	4.6 x 4.9	Fayer et al. 2005	AY741305
C. fayeri	Marsupials	Small intestine	4.3 x 4.9	Ryan et al. 2008 (46)	AF159112
C. macropodum	Marsupials	Small intestine	4.9 x 5.4	Power and Ryan 2008 (47)	AF513227
C. ryanae	Cattle	Small intestine	3.7 x 3.2	Fayer et al. 2008 (48)	AY587166
C. xiaoi	Sheep	Small intestine	3.9 x 3.4	Fayer & Santin 2009 (49)	EU408314
*C. ubiquitum***	Sheep	Small intestine	4.9 x5.2	Fayer et al. 2010 (50)	AF2622328
C. cuniculus	Rabbits	Small intestine	5.4 x 6.0	Robinson et al. 2010 (51)	FJ262725
C. tyzzeri	Mice	Small intestine	4.6 x 4.2	Ren et al. 2012 (52)	AF112571
C. viatorum	Humans	Small intestine	4.7 x 5.4	Elwin et al. 2012 (53)	HM485434
C. scrofarum	Pigs	Small intestine	4.8 x 5.2	Kvac et al. 2013 (54)	EU331243

* Data obtained from Una Ryan and Lihua Xiao 2013 (33); ** indicates that those species also can infect human.

C. varanii (Pavlasek et al. 1995); three in birds, *C. meleagridis* (Slavin 1955), *C. baileyi* (Current et al. 1986), and *C. galli* (Pavlasek 1999); eighteen in mammals, *C. muris* (Tyzzer 1907), *C. parvum* (Tyzzer 1912), *C. wrairi* (Vetterling et al. 1971), *C. felis* (Iseki 1979), *C. andersoni* (Lindsay et al. 2000), *C. canis* (Fayer et al. 2001), *C. hominis* (Morgan-Ryan et al. 2002), *C. suis* (Ryan et al 2004), *C. bovis* (Fayer et al. 2005), *C. fayeri* (Ryan et al. 2008), *C. macropodum* (Power and Ryan 2008), *C. ryanae* (Fayer et al. 2008), *C. xiaoi* (Fayer and Santin 2009), *C. ubiquitum* (Fayer et al. 2010), *C. cuniculus* (Robinson et al. 2010), *C. tyzzeri* (Ren et al. 2012), *C. viatorum* (Elwin et al. 2012), *C. scrofarum* (Kvac et al. 2013) (25,31,33) (Table 1.1). Additionally, there are over 40 genotypes that require more morphological, biological, and molecular data to determine whether they are valid new species (33).

1.3 Morphology and life cycle

The whole life cycle of *Cryptosporidium* spp. contains 6 developmental stages. Various stages have different morphological features as revealed by light and electron microscopic studies.

1.3.1 Oocysts

The oocysts of *Cryptosporidium* spp. are round to oval in shape, with sizes ranging from 3.7 to 8.4 μm in length and 3.2 to 6.3 μm in width (17,48). Oocysts are resistant to chlorine at concentrations typically used in water treatment (55), which is mainly due to its tough, durable oocyst wall structure. *Cryptosporidium* oocyst wall has

four layers, including an outer electron-dense layer (8.5 ± 0.6 nm), a translucent middle layer (4.0 ± 0.2 nm), and two inner electron-dense layers (13.0 ± 0.5 nm and 18.6 ± 1.6 nm, respectively) (56,57). A special suture structure is embedded in the inner layers, which will open during excystation to release sporozoites (56). Each mature oocyst contains four sporozoites, and one membrane-enclosed residual body with large lipid body inside.

1.3.2 Sporozoites and merozoites

Sporozoites and merozoites are two infectious cell forms, which can invade host cells to start the infection. Sporozoites are contained in mature occysts and released by an excystation process after appropriate hosts ingests them. Merozoites are formed in meront developed in host cells, and will be released when meront are mature. Sporozoites and merozoites are morphologically similar, crescent in shape, with the anterior end slightly pointed and the posterior end rounded. In the anterior region, there is an apical complex consisting of a set of organelles including apical rings, conoids, rhoptries, micronemes, and electron-dense granules.

1.3.3 Trophozoies

Trophozoites are transitional forms from sporozoites or merozoites to meronts. After sporozoites or merozoites attach and invade into host cells, the parasites become spherical, which are called trophozoites. Trophozoites are round or oval shaped and vary in size ranging from 2.0 to 2.5 μm (58). During the formation of a trophozoite, its apical complex starts to disappear, and parasitophorous vacuole membrane (PVM) extends

from host cell cytoplasmic membrane until it fully covers the trophozoite. In the trophozoite stage, a unique feeder organelle is formed above the electron-dense attachment zone at the contact site in host cells. Another significant character of trophozoite is the large nucleolus (1.0 - 1.3 μm in diameter) within a large nucleus (57,58).

1.3.4 Meronts

Cryptosporidial trophozoites will undergo asexual cell cycle (merogony) to form multinuclear meronts. The first generation of meronts derived from sporozoites are type I meronts. Merozoites exit from type I meronts, re-infect new host cells, and develop into either type I or type II meronts. Both types I and II meronts are morphological similar (4-5 μm in diameter), except that a mature type I meront produces 6 or 8 merozoites, while a type II meront typically contains 4 merozoites (16). Type I merozoites may enter one or more cycles of mergony before developing into type II meronts.

1.3.5 Gamonts and gametes

Type II merozoites invade new host cells and undergo sexual development to form gamonts (59). Gamonts further develop into microgamonts (male) or macrogamonts (female). A microgamont has a very compact nucleus and lacks rhoptries, which differentiates it from a meront (16). Mature microgamont may contain up to 16 bullet-shaped microgametes, which have slightly expanded anterior ends and relatively big nuclei. Unlike microgamonts, a mature macrogamont contains only one

macrogamete. An early stage of macrogamont is morphologically similar to a trophozoite, and possesses a large nucleus and a feeder organelle (60). However, a later stage of macrogamont is ultrastructurally distinguishable from other developmental stages by possessing amylopectin-like bodies near the feeder organelle, and oocyst wall forming bodies (16).

1.4 Life cycle

Cryptosporidium species complete their life cycle in a single host including both sexual and asexual developments. There are six major development stages as described above, among which only the oocyst is an exogenous stage for the transmission of parasites between hosts (16,60) (Figure 1.1).

The infection is acquired when a susceptible host ingests oocysts from contaminated food or water. The excystation occurs when ingested oocysts are exposed to suitable environmental factors, such as appropriate pH, temperature, pancreatic enzymes, and bile salts (61,62), by which infective sporozoites are released from oocysts through an open suture in the oocyst wall (63). The released motile sporozoites will rapidly attach to and invade gastrointestinal epithelial cells to start intracellular development. During invasion, the sporozoite is encapsulated by host cell membrane that forms a parasitophorous vacuole (PV), in which it develops into a spherical-shaped trophozoite (64,65). The trophozoite enters first generation of merogony to form type I meront containing 8 to 16 haploid merozoites. Released type I merozoites infect neighbor host cells to enter second generation of merogony, forming type II meront

Figure 1.1 Life cycle of *Cryptosporidium parvum* (Reproduced from http://www.cdc.gov/parasites/crypto/biology.html). The infection begins with the ingestion of thick-walled oocysts by host❶. Following excystation in host intestine, sporozoites (a) attach and invade the epithelia cells to form trophozoite (b). Trophozoite develops to type I meront(c), and eight type I merozoites (d) release from mature meront. Type I merozoite infects the epithelia cells, which either develops to type I meront again or to type II meront (e) with four merozoites. The sexual stage starts with type II merozoite (f) invading host cells, and then forming macrogamont (male) (h) and microgamont (female) (g). Upon the fertilization between macrogamont and micorgamete that released from microgamont, a zygote (i) forms and then develops into oocyst. Thin-walled oocysts (j) can directly excyst and cause autoinfection. Thick-walled oocysts (k) are excreted from the host with feces❷, which may cause water and food contamination❸.

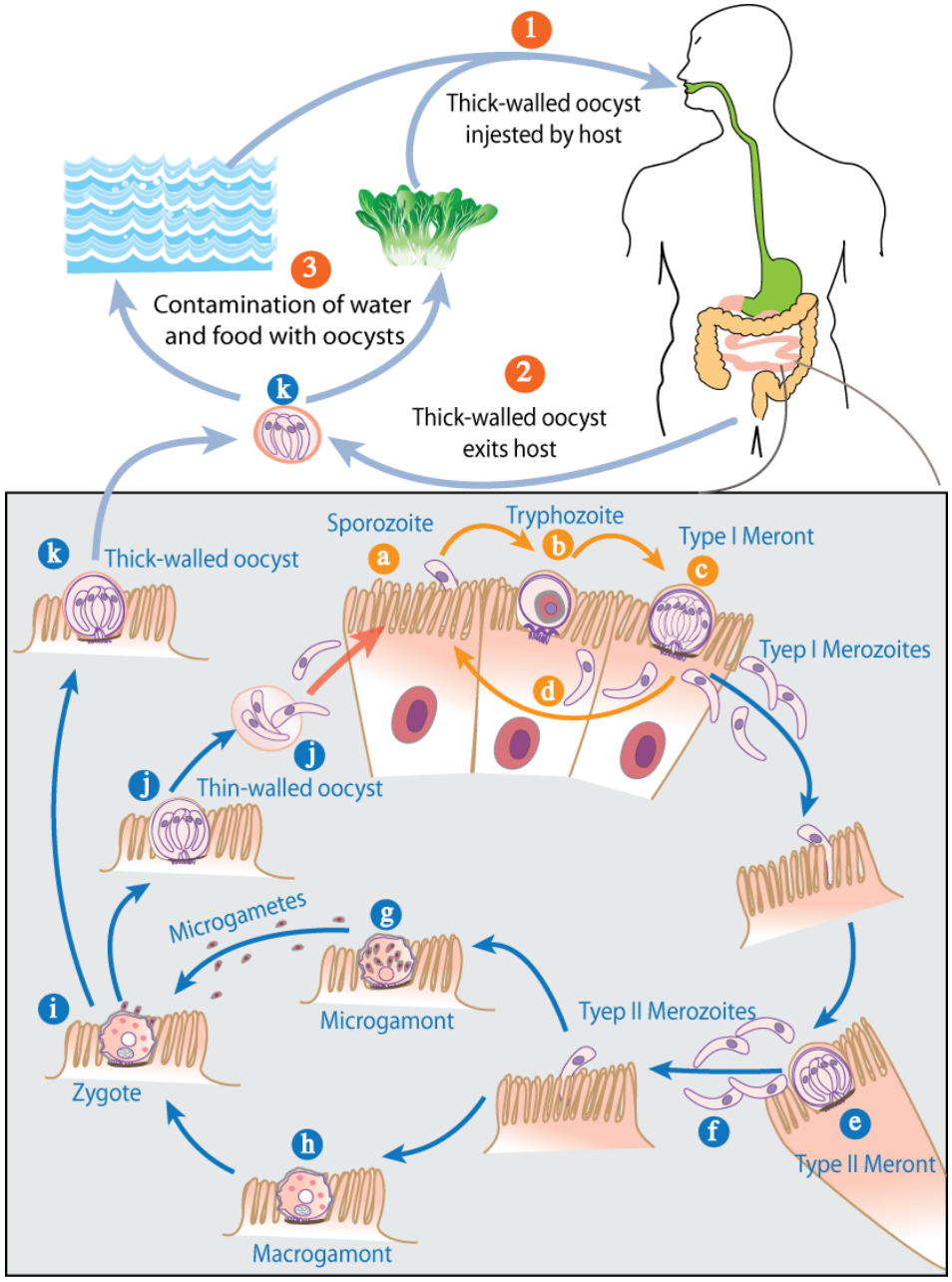
1
Thick-walled oocyst
injested by host
3
Contamination of water
and food with oocysts
2
Thick-walled oocyst
exits host
k
Thick-walled oocyst
Sporozoite
a
Tryphozoite
b
Type I Meront
c
Tyep I Merozoites
d
j
Thin-walled oocyst
Microgametes
g
Microgamont
Tyep II Merozoites
i
Zygote
f
e
Type II Meront
h
Macrogamont

containing four merozoites. Type II merozoites invade new host cells and initiate sexual reproduction to form either microgamonts or macrogamonts. Microgametes, which developed in the microgamonts, are released to search for uninucleate macrogamonts. Fertilization between micro- and macro-gametes forms zygotes that are the only diploid cells in the complex life cycle of *Cryptosporidium*. A zygote immediately undergoes sporogony to form an oocyst containing 4 haploid sporozoites. There are thick- and thin-walled oocysts. Approximately 80% of the oocysts have a thick, two-layer wall. These thick-walled oocysts are released into the environment. The other 20% of the oocysts contain one layer thin-wall, which can be ruptured to release sporozoites within the same host, causing auto-infection. The auto-infection of sporozoites from thin-walled oocysts and repetitive type I merogonic development are responsible for the persistent and chronic infections, particularly in immune-deficient individuals without repeated exposure to the environmental oocysts (16).

1.5 Cryptoporidiosis

Cryptosporidiosis is a common diarrheal illness caused by *Cryptosporidium* infection. *Cryptosporidium* typically infects epithelial cells in the microvillus border of the gastrointestinal tract of all classes of vertebrates, including fishes, amphibians, reptiles, birds and mammals. Although a number of *Cryptosporidium* species can infect humans, *C. parvum* and *C. hominis* are the two major human pathogens. Cryptosporidiosis is generally self-limiting in immunocompetent individuals (66). However, it may result in fulminant and/or chronic diarrhea, or even death in

immunocompromised patients, as well as persistent infections and stunted mental development in children (67,68). In developing countries *Cryptosporidium* is one of the four leading diarrheal pathogens in children under 2 years of age (69). Moreover, cryptosporidiosis is highly associated with malnutrition in children or even mortality in toddlers, and the infections in infants and toddlers are also linked to impairing of growth, physical fitness, and cognitive function in late childhood (69-71).

1.6 Host immune responses

The host immune system plays a critical rule in controlling the pathological and clinical outcomes associated with the *Cryptosporidium* infections. Cryptosporidiosis is usually self-limiting in immunocompetent individuals, but can be chronic and life-threatening in immunocompromised patients, which suggests that host immune status is critical in eliminating *Cryptosporidium* infections. Although both innate and adaptive immune responses in humans and animals are involved, innate immunity alone appears to be insufficient to protect hosts from cryptosporidial infections (72,73). Here we will highlight the roles of major immune factors in response to cryptosporidial infections in humans and animals.

1.6.1 $CD4^+$ and $CD8^+$ T cells

Several studies have suggested that $CD4^+$ T cells are the most important cells in the immune response to *Cryptosporidium* infection. The clinical outcome of cryptosporidiosis is highly correlated to the $CD4^+$ cell count. In human patients whose

$CD4^+$ cell counts are over 180 cells/μl, including those carrying immunodeficiency virus (HIV), cryptosporidiosis is generally self-limited. However, in patients with lower $CD4^+$ cells counts (e.g., <50 cells/μl), such as AIDS patients, the infection become chronic and life-threatening (72,74). Furthermore, the rapid increase of mucosal $CD4^+$ cells is associated with the clearance of intestinal cryptosporidiosis in a HIV-infected patient during highly active antiretroviral therapy (75). Similar results have also been observed in mice. Cryptosporidial infections in nude mice (T cell deficient) are chronic, suggesting that T cells are required for the recovery from *Cryptosporidium* infection (76). Mice with severe combined immunodeficiency (SCID) lack both $CD4^+$ and $CD8^+$ T lymphocytes and experience persistent life-threatening cryptosporidial infectious after inoculated with *C. parvum* oocysts. When SCID mice were transfered with complete lymphocyte populations (containing both $CD4^+$ T and $CD8^+$ T cells), or $CD4^+$ T cells alone, or $CD8^+$ T cells alone, followed by challenges with *C. parvum*, only those received both $CD4^+$ and $CD8^+$ cells, or $CD4^+$ cells alone, but not those received $CD8^+$ cells alone, could recover from persistent cryptosporidial infections (77-79). Those results suggest that $CD4^+$ T cells, but not $CD8^+$ T cells, are necessary for the eradiation of established *C. parvum* infection. Similarly, the depletion of $CD4^+$ cells in immunocompetent mice exacerbated the *C. parvum* or *C. muris* infections (80,81). The significance of $CD8^+$ T cells in control of cryptosporidiosis is less clear than $CD4^+$ T cells. Some studies showed that $CD8^+$ T cells were not required for control of cryptosporidiosis, while others suggested they might play some non-essential roles in this process. For example, in major histocompatibility complex (MHC) class-I deficient

mice that lacked functional $CD8^+$ T cells, investigators observed a similar level of *C. parvum* infection to that in wild-type mice (82). On the other hand, another study showed that the depletion of $CD8^+$ cells from donor spleen cells delayed the recovery of the reconstituted SCID mice from parasites infection (78). Additionally, the depletion of $CD8^+$ cells could reduce the level of protection to *C. muris* infection, and the blocking of $CD8^+$ cells with antibodies could increase *C. muris* oocyst shedding in mice (80).

1.6.2 B cells

The roles of B cells and antibodies in cryptosporidiosis are still not fully understood. The correlation between selective IgA deficiency and persistent cryptosporidial infection indicated that B cells contributed to the elimination of parasites (83). The high serological responses to a 27-kDa *Cryptosporidium*-antigen was associated with a reduced risk of diarrhea in both HIV-negative and HIV-positive patients, also suggesting that antibodies played protective roles (84,85). However, some other evidence indicated that antibodies might not play an essential role to protect host from or eliminate *Cryptosporidium* infection. For example, *Cryptosporidium*-specific antibody levels seemed to be uncorrelated to the diarrheal symptom (86). High levels of parasite-specific antibodies were also present in AIDS patients with chronic cryptosporidiosis (87). The nonessential roles of B cells in the recovery from *Cryptosporidium* infection were also observed in mice (88,89).

1.6.3 IFN-γ

A number of studies using SCID and nude mice suggested that IFN-γ played a major role in the innate immunity against *C. parvum* infections. Both SCID and nude mice were relatively resistant to *C. parvum* infection, but treatment with anti-IFN-γ neutralizing antibodies could significantly decrease the resistance, indicating that IFN-γ was involved in a T-cell-independent immune response to the parasite infection (78,81). Similarly, *C. parvum* infections were much heavier in IFN-γ knockout SCID mice than parent SCID mice (90).

IFN-γ is also a key player in adaptive immune responses. An in vitro study showed that $CD4^+$ T-cells purified from *C. parvum* immunized mice could produce IFN-γ upon incubation with *C. parvum* antigen (91). Treatment of normal BALB/c mice with anti-IFN-γ antibodies greatly increased reproduction of *C. parvum* oocysts, although infection was self-limited (81). Additionally, IFN-γ knockout adult BALB/c mice developed moderate *C. parvum* infection and recovered later, whereas infection in IFN-γ knockout adult C57BL/6 mice could be overwhelming and might cause death within two weeks after infection (92,93). Furthermore, the high levels of IFN-γ in the intestines were associated with the recovery from *C. parvum* infection in neonatal mice (94), calves (95,96), and humans (97).

1.6.4 IL-12

Interleukin 12 (IL-12) is another important cytokine that induces NK cells and T cells to produce INF-γ (98) in response to the *C. parvum* infection. Treating immunocompetent or immunodeficient neonatal BALB/c mice with a single dose of IL-

12, one day before the inoculation with *C. parvum* oocysts, prevented the establishment of infection (99). The protective role of IL-12 was associated with IFN-γ production. The IL-12 treatment increased the levels of IFN-γ mRNA in the intestines, and injection of anti-IFN-γ antibodies into mice two days prior to the IL-12 treatment completely blocked the protective effect of IL-12 against *C. parvum* infection (99). In the early stage of infection in BALB/c mice, anti-cryptosporidial resistance was associated with the strong expression of IL-12 and IFN-γ mRNA in the intestines (100). Furthermore, *C. parvum* infections would result in acute diseases in the IL-12 knockout adult C57BL/6 mice, though the mice were able to fully recover within 2 weeks, whereas infections could not be established in the wild-type adult mice (101). Therefore, IL-12 knockout C57BL/6 mice are also used as a model for testing drug efficacies against acute cryptosporidiosis.

1.7 Treatments

In the past few decades, at least hundreds of chemo- and immunotherapeutic agents have been tested in vitro or in vivo for their anti-cryptosporidial efficacies, and some of them have been tested in clinical trials (102). However, fully effective anti-cryptosporidiosis drugs are still not available today. Currently, only nitazoxanide is approved by FDA to treat cryptosporidiosis in immunocompetent patients, but its efficacy is still under debate. Here we will briefly review the current status of anti-cryptosporidial drug development as well as the recommended treatments and medicines.

1.7.1 Highly-active anti-retroviral therapy

Although highly-active anti-retroviral therapy (HAART) is an aggressive treatment regimen to suppress HIV viral replication and the disease progression, HAART could also markedly decrease occurrence of opportunistic infections including cryptosporidiosis in AIDS patients. Since the introduction of HAART in 1996, the mortality and morbidity caused by opportunistic pathogens in AIDS patients have decreased dramatically in developed countries (103). An earlier survey of 6,941 HIV-infected individuals in Europe and Australia showed that cases of cryptosporidiosis decreased over 15 times since HAART was available (1997 - 2001) in comparison with those in the pre-HAART era (1994-1996) (104). HAART can improve cryptosporidiosis symptoms and even completely eradiate the parasite from AIDS patients. The anti-cryptosporidial effect of HAART was associated with the reconstruction of cellular immunity and the increase of $CD4^+$ T-cells (103). In addition to rebuilding host immunity, protease inhibitors used in HAART also displayed certain chemotherapeutic effect against *Cryptosporidium* infection (105-107). Protease inhibitors in HAART are known to target HIV-1 aspartyl protease, but their therapeutic mechanism against *Cryptosporidium* is yet unclear.

1.7.2 Paromomycin

Paromomycin is a non-absorbable aminoglycoside with broad spectrum of antimicrobial activity, which is mainly used to treat *Giardia* and amoebic intestinal infectious. In the early 1990s, the anti-cryptosporidiosis activity of paromomycin was reported in a number of studies (108-111). Since then, paromomycin was widely used to

treat cryptosporidiosis in HIV-infected patients. However, a later study on 35 AIDS patients indicated that paromomycin did not show better efficacy than placebo in treating symptomatic cryptosporidial enteritis (112). Paromomycin is still considered as an option to treat cryptosporidiosis in AIDS patients in many countries, although it is not "officially" approved by FDA. Because of the clinical significance of cryptosporidiosis, paromomycin may be used in adult AIDS patients along with HAART, but is not recommended to be used alone without HAART (http://aidsinfo.nih.gov/guidelines) (113).

1.7.3 Nitazoxanide

Nitazoxanide is the only FDA-approved drug for treating cryptosporidiosis in patients with a healthy immune system, but not in immunocompromised individuals. In an earlier study, administration of nitazoxanide for 3 days at 500 mg for adults or 10 mg for children twice daily significantly reduced the duration of both diarrhea and oocyst shedding in immunocompetent patients in comparison to placebo (114). Among AIDS patients, nitazoxanide was effective in eradicating *C. parvum* and resolving the associated diarrhea in adults (115), but ineffective in children in two randomized trials, even with high doses and prolonged treatments (116,117).

The introduction of HAART has tremendously decreased the negative effects of cryptosporidiosis on the HIV-infected patients in developed country. However, development of new inexpensive and effective therapeutics for cryptosporidiosis is still necessary. First, the availability of antiretroviral drugs is highly limited in the low and middle-income countries. In 2012, the World Health Organization (WHO) estimated that

only 33% of children (0 - 14 years old), among eligible for receiving HAART treatment groups, have received HAART in the 22 priority countries in the Global Plan of WHO (118). Second, cryptosporidiosis is one of the main causes of diarrhea in young children that is independent on the HIV infections (119). Cryptosporidial infections in children could result in impaired physical fitness in late childhood (120), or even childhood deaths as reported in sub-Saharan Africa (121). Third, *Cryptosporidium* frequently causes water-borne outbreaks, and is listed as a Category B priority pathogen in the Biodefense program in the United States. Fully effective treatments are urgently needed when massive cryptosporidiosis outbreaks occur. Development of effective chemotherapy for cryptosporidiosis is particularly necessary in developing countries, in which chronic diarrhea and malnutrition caused by cryptosporidiosis are common in children.

1.8 Fatty acid metabolism in *Cryptosporidium*

The availability of the whole genomes of *C. parvum* and *C. hominis* has greatly contributed to our understating of *Cryptosporidium* metabolism. The annotation and analysis of their whole genomes have revealed a highly streamlined metabolism in these two major human *Cryptosporidium* species. More importantly, *Cryptosporidium* are unable to synthesize most nutrients de novo, including amino acids, nucleotides and fatty acids. Additionally, *Cryptosporidium* lacks a plastid-derived apicoplast as well as the mitochondrial genome and associated metabolic pathways (11,12,18). Therefore, many well-studied drug targets in other apicomplexans are absent in *Cryptosporidium*.

The lack of typical drug targets is one of the major reasons for the remarkable insensitivity of *Cryptosporidium* to various antimicrobial agents. However, a number of unique drug targets in different metabolic pathways have been proposed and investigated, such as the synthesis of longer isoprenoid using 5-carbon isoprene units (122), dihydrofolate reductase (123), pyrimidine salvaging enzymes (124), inosine monophosphate dehydrogenase (125), and fatty acids metabolic pathways (126). In this section, we will highlight the major features of fatty acid metabolism in *Cryptosporidium.*

Fatty acid metabolism in *C. parvum* is highly simplified, featured by the lack of de novo fatty acid synthesis and β-oxidative pathway. However, this parasite possesses a number of other enzymes involved in lipid metabolism, including those involved in fatty acids activation and elongation, and synthesis of complex lipids (127,128). This parasite possesses two fatty acid elongation systems, namely type I fatty acid synthase (CpFAS1) and long chain fatty acid elongase system. *CpFAS1* is a 25-kb intronless gene that encodes a multifunctional polypeptide compromised of at least 21 enzymes domains, including N-terminal loading unit containing an acyl-ligase (AL) and an acyl-carrier protein (ACP), C-terminal reductase (R) domain, and three internal acyl-elongation modules (129,130). Each internal acyl-elongation module contains a complete set of 6 enzymes including ACP, acyl-transferase (AT), ketoacyl-CoA synthase (KS), ketoacyl-ACP reductase (KR), hydroxyacyl-ACP dehydrase (DH), and enoyl-ACP reductase (ER) for the elongation of two-carbon units (131). Biochemical data demonstrated that N-terminal AL domain and C-terminal reductase had a substrate preferences towards long

chain fatty acids and very long chain fatty acyl-chains, separately, indicating that the CpFAS1 is involved in fatty acid elongation rather than de novo synthesis of fatty acids (129,131). In addition to CpFAS1, *C. parvum* possesses another fatty acid elongation system that uses fatty acyl-CoA thioesters rather than fatty acyl-ACP as substrates. All enzymes involved in the elongation of fatty acyl-CoA thioesters are present in the *C. parvum* genome, including β-ketoacyl-CoA synthase (cgd8_4630), β-ketoacyl-CoA reductase (cgd3_2370), β-hydroxyacyl-CoA dehydratase (cgd3_2150) and trans-2-enoyl-CoA reductase (cgd2_1200) (132). The biochemical features of β-ketoacyl-CoA synthase (also known as fatty acyl elongase) in *C. parvum* have been characterized using recombinant protein expressed in HEK-293T cells. This elongase was capable of adding a single two-carbon unit to long chain fatty acyl-CoA thioesters with a substrate preference towards myristoyl-CoA (C14:0) and palmitoyl-CoA (C16:0) (133).

A long-type fatty acyl-CoA binding protein (ACBP) has also been identified in *C. parvum*. ACBP may function as an acyl-CoA ester carrier and responsible for intracellular movement of activated fatty acids or restraining them to prevent free acyl-CoA esters from disrupting cell membranes. Although ACBPs are capable of binding medium- to long-chain fatty acyl-CoA esters, different ACBPs have their own substrate preferences and binding affinities. In line with *C. parvum* elongase, CpACBP also prefers to binding to long chain and very long chain fatty acyl-CoA (127).

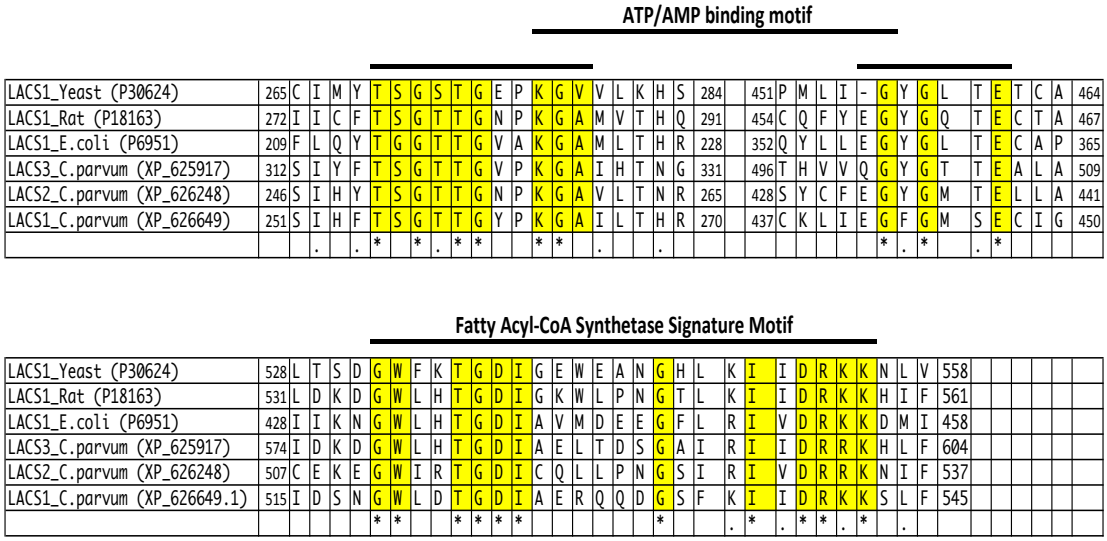

Figure 1.2 Comparison of amino acid sequences at the two conserved signature motifs of ACSs from *C. parvum* and other species. Highly conserved amino acids are highlighted in yellow. Position of the first and last residues is indicated. Identical and highly similar amino acids are marked by asterisks (*), and dots (.), respectively.

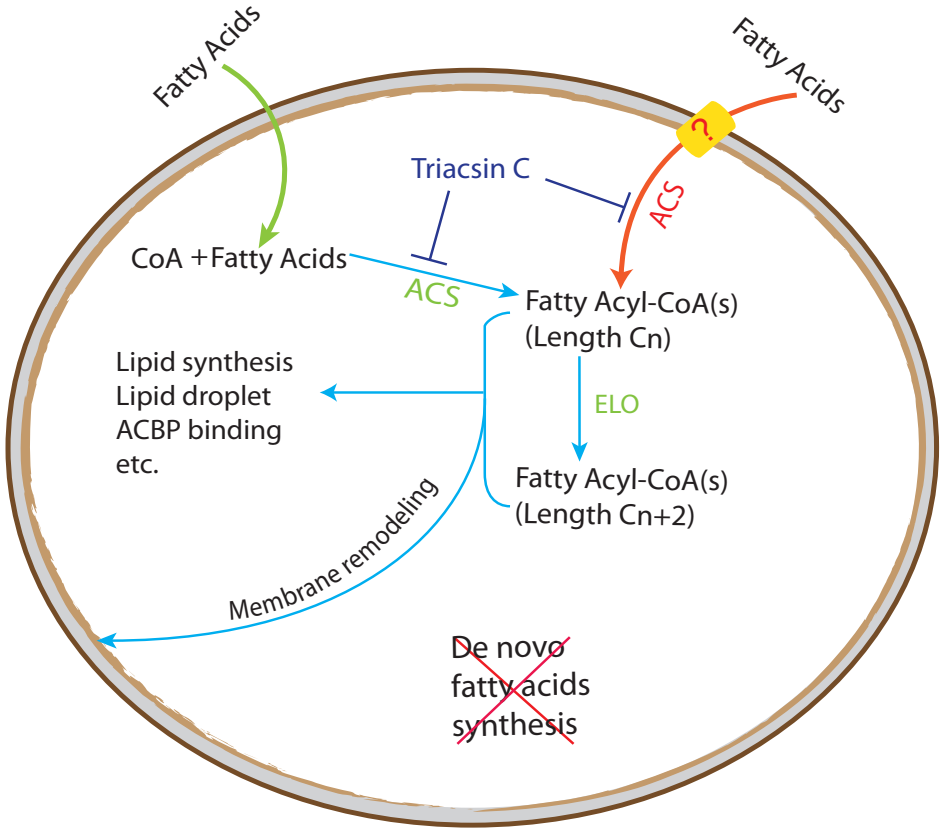

Figure 1.3 Illustration on the role of ACS in the fatty acid metabolism in *C. parvum.* The parasite is incapable of synthesizing fatty acids de novo, thus relying on salvaging them from the environment or host cells. Fatty acids cross the biomembranes either by unknown transporters and/or coupled with acylation by ACS, or by passive diffusion. Free fatty acids need to be activated by ACS to form fatty acyl-CoA before they enter subsequent metabolism pathways, including further chain elongation by elongase (ELO), synthesis of complex lipids and membrane remodeling. Inhibition of ACS function (such as by triacsin C) may completely block these pathways, thus killing the parasite.

C. parvum also possesses three long chain fatty acyl-CoA synthetases (CpACSs; also known as fatty acid-CoA ligases, ACLs) [EC 6.2.1.3] that catalyze the thioesterification between free fatty acids and CoA to form fatty acyl-CoAs (134). Virtually all fatty acids need to be activated to form fatty acyl-CoAs before they can enter subsequent metabolic pathways, such as the synthesis of complex lipids and the degradation of fatty acids via the β-oxidation (135). Fatty acyl-CoAs are also involved in other biological processes such as protein modification (136,137), cell proliferation (138), intracellular protein transport (139), and cell signaling (140,141). Some ACSs are involved in fatty acid transport into cells by the process of vectorial acylation (142,143). Therefore, ACSs are indispensible in all organisms and may serve as good drug targets.

All of the three CpACSs contain a highly conserved AMP/ATP binding motif and an ACS signature motif essential to the ACS activity (142,144) (Figure 1.2). ACS proteins from different taxonomic groups, such as those from humans (e.g., P33121), yeast (e.g., P30624) and bacteria (e.g., P69451), share less than 50% similarities. Based on the C. parvum and C. hominis genome information and related studies, CpACSs might be involved in salvaging fatty acids from environment and/or from host cells as some ACSs in bacteria and yeast (145,146). Their products would be routed to many critical metabolic pathways including the fatty acid elongation, lipid synthesis, membrane remodeling, and lipid droplet forming (128,147) (Figure 1.3). Therefore, we hypothesize that targeting CpACSs may have the potential to block all downstream reactions using fatty acids as substrates, thus inhibiting the parasite growth.

To test the hypothesis, we have studied the molecular and biochemical features of CpACSs. We have also tested the effect of a potent ACS inhibitor, triacsin C, on CpACS1 and CpACS2 enzyme activities, as well as its efficacy against parasite development in vitro on HCT8 cells and in vivo in an IL-12 knockout mouse model representing acute cryptosporidiosis.

2 LONG CHAIN FATTY ACYL-COENZYME A SYNTHETASES AS NOVEL DRUG TARGETS IN *CRYPTOSPORIDIUM PARVUM*[*]

2.1 Overview

C. parvum is a unicellular zoonotic pathogen that can cause severe watery diarrhea in both humans and animals (66). Cryptosporidial infections in immunocompromised individuals can be prolonged and life threatening. However, in the United States, FDA-approved treatments remain unavailable to treat this opportunistic infection in AIDS patients, whereas only nitazoxanide is approved for use in immunocompetent individuals. Therefore, there is an urgent need for new drugs, particularly those that can be safely used in immunocompromised people. The slow progress in developing anti-cryptosporidial drugs is largely due to the unique metabolic features in this parasite, which are represented by a highly streamlined metabolism and inability to synthesize nutrients de novo (11,18). In addition, as previously mentioned, this parasite is metabolically different from other apicomplexans by lacking many important pathways, including type II fatty acid synthase (FAS), isoprenoid synthesis, the cytochrome-based respiratory chain and the citrate cycle (11). Therefore, many classic drug targets are not effective against *Cryptosporidium*. So, there is an urgent need

---

[*] Part of this research was reprinted from Fengguang Guo, Hiali Zhang et al. 2014, Amelioration of *Cryptosporidium parvum* Infection In Vitro and In Vivo by Targeting Parasite Fatty Acyl-Coenzyme A Synthetases. *Journal of Infectious. Disease*. 209(8): 1279-1287, with permission from Oxford University Press. It is available online at: http://jid.oxfordjournals.org/content/209/8/1279.long.

to identify novel drug targets which can be used to develop new anti-*Cryptosporidium* drugs, particularly new drugs for AIDS patients.

However, some essential core metabolic pathways, including energy metabolism and lipid synthesis are present in this parasite. Many essential enzymes within these pathways may serve as new drug targets because they are either absent in, or highly divergent from those in humans and animals. Within lipid metabolic pathways, [AMP-binding]-long chain (LC) and very long chain (VLC) fatty acyl-CoA synthetases (ACSs; aka, fatty acid-CoA ligases, ACLs) [EC 6.2.1.3] are a large family of enzymes that catalyze the thioesterification between free fatty acids and CoA to form fatty acyl-CoAs via a two-step reaction (Figure 2.1) (134). ACS may also function as fatty acid transporters in some organisms (142,143). ACS is indispensible in all organisms because fatty acids have to be activated by this enzyme to form acyl-CoA thioesters before they can enter various catabolic and anabolic pathways. Fatty acyl-CoA thioesters serve as key intermediates in the biosynthesis of cellular lipids and in energy metabolism via β-oxidation (135). Additionally, acyl-CoAs are also involved in some biological processes such as protein modification (136,137), cell proliferation (138), intracellular protein transport (139), and cell signaling (140,141).

The *C. parvum* genome encodes three LC-ACSs (named CpACS1, CpACS2 and CpACS3), which differs from other apicomplexans such as *Plasmodium falciparum* that possesses at least 11 ACS genes (148). In the present study, we have cloned and engineered all three CpACS genes into the pMAL-c2x vector. We successfully expressed recombinant CpACS1 and CpACS2 as maltose-binding protein (MBP)-

fusions proteins and analyzed their biochemical characters. We provided detailed enzyme kinetics and demonstrated that triascin C, a potent ACS inhibitor, not only inhibited CpACS enzyme activity, but also displayed satisfactory efficacies against *C. parvum* growth both in vitro and in vivo.

2.2 Materials and methods

2.2.1 General procedures for manipulating C. parvum and isolating nucleotide acids

The IOWA-1 strain of *C. parvum* maintained by infecting calves was purchased from Bunch Grass Farm (Deary, ID) and only fresh oocysts (≤3 months old since harvest) were used in this study. Oocysts were purified from calf feces by a sucrose-gradient centrifugation protocol, followed by treatment with 10% Clorox on ice for 7 min, and repeatedly washing by centrifugation in sterile water for 5-8 times (149,150). If minor debris was still present, oocysts were further purified by a Percoll-gradient based method and resuspended in phosphate-buffered saline (PBS) before use. For the preparation of free sporozoites, oocysts were excysted in PBS containing 0.25% trypsin and 0.75% taurodeoxycholic acid for 1 h at 37 °C. Sporozoites were washed 2-3 times with HBSS and concentrated as previously described (151).

For in vitro experiments, a human ileocecal epithelial cell line (HCT-8, ATCC # CCL-225) was seeded into 24-well cell culture plates and cultured at 37 °C in RPMI 1640 medium (Sigma-Alderich) containing 10% fetal bovine serum (FBS) under an atmosphere of 5% CO_2 until they reached to ~80% confluence. Purified *C. parvum*

oocysts were added into the cell culture, typically at a parasite:host cell ratio of 1:2 (i.e., 10^5 oocysts/well) or as specified, and allowed to infect host cells for 3 h. Parasites that failed to invade host cells were removed by a medium exchange. Intracellular parasites were allowed to grow for specified time periods before subsequent experiments including RNA isolation for expression analysis or fixation for immunofluorescence staining.

For the cloning of CpACS genes, genome DNA (gDNA) was isolated from oocysts or sporozoites using DNeasy Blood & Tissue Kit (Qiagen Inc., Valencia, CA). For gene expression analysis and qRT-PCR-based in vitro drug testing, total RNA was isolated from oocysts, free sporozoites or intracellular parasites developed in host cells at specified times using Qiagen RNeasy Mini Kit as described (150).

2.2.2 Sequence analysis

Phylogenetic relationships of CpACS proteins with other orthologs within the chromalveolates were determined by maximum likelihood (ML) and Bayesian inference (BI) methods. ACS orthologs were retrieved from NCBI protein databases by repeated BLAST searches using ACS protein sequences from *C. parvum* and other apicomplexans as queries. Multiple sequence alignments were performed using MUSCLE v3.8.31 program (http://www.drive5.com/muscle/). Identical sequences and short partial sequences were removed, and only amino acid positions that could be unambiguously aligned were used in phylogenetic reconstructions. The final dataset consisted of 120 taxa with 281 amino acid positions. In ML analysis, bootstrapping supporting values were derived from 1000 replicated sequences using TreeFinder

program (version 2008) (http://www.treefinder.de). BI analysis used MrBayes program (v3.2.1) (http://mrbayes.sourceforge.net/), in which 10^6 generations of searches were performed with two independent runs, each run with 4 chains running simultaneously. Posterior probability (PP) values were derived after the first 25% trees were discarded. Both ML and BI analyses used WAG amino acid substitution model, with the consideration of the fraction of invariance ($\boldsymbol{F}_{\mathbf{inv}}$) and a 4-rate gamma distribution among varied sites ($\boldsymbol{\Gamma}_{\mathbf{[4\text{-}rate]}}$) for among-site heterogeneity (i.e., $\boldsymbol{F}_{\mathbf{inv}} + \boldsymbol{\Gamma}_{\mathbf{[4\text{-}rate]}} + \boldsymbol{WAG}$). Consensus trees were displayed using FigTree (v1.3.1) program (http://tree.bio.ed.ac.uk/software/figtree/), and final annotation was performed using Adobe Illustrator CS4 program.

Sequence logos for the conserved motifs were derived from the 120 aligned chromalveolate sequences using WebLogo3 server (http://weblogo.threeplusone.com). Potential signal peptides were analyzed at SignalP 4.1 server (http://www.cbs.dtu.dk/services/SignalP/) using model for eukaryotes.

2.2.3 Quantitative analysis of CpACS gene expressions

The relative expression levels of *CpACS1, CpACS2* and *CpACS3* genes in oocysts, sporozoites and intracellular parasite developed in HCT-8 cells for 6 h to 72 h were evaluated by quantitative real-time RT-PCR (qRT-PCR) using One-Step RT-PCR QuantiTect SYBR Green RT-PCR Kit (Qiagen). The levels of *C. parvum* 18S rRNA (Cp18S) were used as the internal standard for normalization as previously described (152). Each of the qRT-PCR reaction contained 0.5 μM of primers, 1 ng of total RNA from oocysts and sporozoites or 15 ng total RNA from intracellular parasites in 20 μL

Table 2.1 List of primers used in this study.

Gene	Direction	Sequence of primer pairs (5' – 3') *	Product size (bp)	Application
CpACS1	Forward	gtatatggatccATGGAAGAGAAAATCGACA	2058	Expression
	Reverse	ccacgatctagaTCAAATTTGTGATCTTAAAG		
CpACS2	Forward	gaattaggatccATGGGGAACATTACTTCA	2052	Expression
	Reverse	gaacaatctagaTCATTCATTCTTAGGTTTTGAG		
CpACS3	Forward	gaaataggatccATGAAGATTCTAAGATTAGC	2302	Expression
	Reverse	gaaccatctagaTCATAGCTTATTTCCTAATT		
CpACS1	Forward	GCAGAAAGACAACAAGATGGC	102	qRT-PCR
	Reverse	TCCCTCAATTCTTTCTGGTGA		
CpACS2	Forward	TATATGGGTGTTAGGGTGCCA	127	qRT-PCR
	Reverse	CCTGGACTGCTCCAATATGAA		
CpACS3	Forward	TGGTGTCCAGGTTTCACTTTC	96	qRT-PCR
	Reverse	TTCAATTCACCAAGCCTCATC		
Cp18S	Forward	TTGTTCCTTACTCCTTCAGCAC	175	qRT-PCR
	Reverse	TCCTTCCTATGTCTGGACCTG		
Hs18S	Forward	GGC GCC CCC TCG ATG CTC TTA	189	qRT-PCR
	Reverse	CCC CCG GCC GTC CCT CTT A		

* Lowercase letters sequence represents the linker region

volume. The reactions were incubated at 50 °C for 30 min to synthesize cDNA, heated at 95 °C for 15 min to inactivate the reverse transcriptase and then followed by 40 thermal cycles of PCR amplification (95 °C for 20 sec, 58 °C for 30 sec and 72 °C for 30 sec) with a CFX96 Real-Time PCR detection system (Bio-Rad Labs, Hercules, CA). Primers

specific to CpACS genes and 18S rRNA were listed in Table 2.1. Each experimental condition included at least three biological replicates (RNA samples) and two technical replicates (qRT-PCR reactions).

Threshold cycle ($\mathbf{C_T}$) values were used for computing the relative levels of expression, in which data were first normalized by computing the ΔC_T values between CpACS mRNA ($\Delta C_{T[sample]}$) and Cp18S rRNA ($\Delta C_{T[Cp18S]}$) for all samples. PCR amplification efficiencies ($\boldsymbol{\varepsilon}$) for individual genes were determined by equation

$$\varepsilon = 10^{-(\frac{1}{slop})} \qquad (1)$$

in which slops were obtained by real-time qRT-PCR with a serial dilutions of a pooled total RNA sample, followed by linear regression of $\mathbf{C_T}$ values against common logarithms of relative RNA concentrations (dilutions). Two types of relative expression levels were plotted. The first one was the percent levels of mRNA of a specified gene in various samples in relative to the one with the highest level of expression, which was derived from relative fold changes ($\boldsymbol{f}$) determined by equation:

$$f = \varepsilon^{\Delta\Delta C_T} \qquad (2)$$

where $\Delta\Delta C_T$ values were those between a specified sample and the highest one. Second, because the PCR amplification efficiencies for all three genes and Cp18S rRNA were nearly identical (i.e., $\boldsymbol{\varepsilon}$ = 1.896 ± 0.017) (Figure 2.3B), we were able to also use the

$\Delta\Delta C_T$ method to directly compare the relative levels of expressions between the three CpACS genes in all samples against the overall mean.

2.2.4 Molecular cloning and heterogeneous expression

CpACS1, CpACS2 and *CpACS3* genes have been annotated by the *C. parvum* genome-sequencing project (GenBank accession numbers: XM_626649 for ACS1, XM_626248 for ACS2, and XM_625917 for ACS3). Their open reading frames (ORFs) were amplified from *C. parvum* genome DNA by PCR using high-fidelity *Pfu* DNA polymerase (Stratagene) and cloned into a pCR2.1-TOPO vector (Invitrogen). Cloned genes were sequenced to confirm their identities and then subcloned into pMAL-c2x expression vector (New England Biolabs) for expression as maltose-binding protein (MBP)-fusion proteins. Primers used for cloning were also listed in Table 2.1. Plasmids with correct sequences and orientation were transformed into a Rosetta 2 strain of *Escherichia coli* competent cells (Novagen) for protein expression. Briefly, a single colony of transformed bacteria was first inoculated into 50 ml LB media containing ampicillin (50 μg/ml), chloramphenicol (25 μg/ml), and glucose (2 mg/ml), and allowed to grow overnight at 30 °C in a shaking incubator. The overnight cultures were diluted 1:20 with fresh medium and incubated for ~2 h at 37°C until their OD_{600} reached to ~0.5. Then, isopropyl-1-thio-β-D galactopyranoside (IPTG) was added to the cultures at a final concentration of 0.3 mM, and bacteria were allowed to grow for ~16 h under 16 °C to express proteins. The collection of bacterial pellets and purification of MBP-fusion proteins by an amylose resin-based affinity chromatography were followed manufacturer's protocols (New England Biolabs, Ipswich, MA).

2.2.5 Production and affinity purification of anti-CpACS1, anti-CpACS2, and anti-CpACS3 polyclonal antibodies

Polyclonal antibodies against CpACS1, CpACS2 and CpACS3 were commercially produced by Alpha Diagnostic International (San Antonio, TX). Antibodies to CpACS1 was produced using a recombinant protein corresponding to the amino acids from position 99 to 254 in two specific pathogen-free (SPF) rabbits by a standard 63-day protocol, which included 5 injections at multiple sites at 14 day interval. Pre-immune bleed was collected prior to immunization, and two immune bleeds were collected at weeks 7 and 9, separately. For anti-CpACS3 antibody production, a recombinant protein corresponding to the amino acids from position 86 to 288 of CpACS3 was applied to generate anti-CpACS3 polyclonal antibodies in SPF rabbits with same protocol as CpACS1 antibodies producing. Antibodies to CpACS2 was generated in two SPF hen using synthesized peptide CTAAFVYGQLGREGTKLGSN corresponding to amino acids at positions from 271-290 by a standard 63-day immunization protocol, including isolation of chicken IgY from 6 egg yolks.

Antibodies were subjected to an antigen-based affinity purification procedure using a previously described protocol with minor modification (153), Briefly, for CpACS1or CpACS3 antibodies, the recombinant CpACS1 or CpACS3 antigens were separated by SDS-PAGE and transferred onto nitrocellulose membranes. The blots were stained with Ponceau Red and the strips containing the recombinant proteins were cut out for subsequent antibody purification. For CpACS2 antibodies purification, synthetic peptide was directly blotted onto nitrocellulose membranes and air-dried. All membranes

were blocked with 5% BSA in TBST (Tris-buffered saline containing 0.02% Tween 20) for 1 h, and then incubated separately with anti-CpACS1 or anti-CpACS3 sera, or anti-CpACS2 IgY overnight at 4 °C on an orbital shaker. The blots were washed three times with TBST (10 min each), and purified antibodies were eluted in 0.2 M Glycine (pH 2.2) by vigorous shaking on an orbital shaker for 2 minutes, and then quick neutralized with 1 M Tris-HCl (pH 7.6) buffer.

2.2.6 Immunofluorescence microscopy

Free sporozoites were prepared by an in vitro excystation procedure, in which *C. parvum* oocysts were incubated in PBS containing 0.5% taurodeoxycholic acid (TDC) and 0.25% trypsin for 45 minutes at 37 °C. Freshly released sporozoites were collected and washed with culture medium containing 10% fetal bovine serum (FBS) to neutralize trypsin. Type I merozoites were collected from the supernatants of cultured HCT-8 cells infected with *C. parvum* for 12-18 h. Different intracellular stages of parasites were obtained by infecting HCT-8 cell monolayers cultured on glass coverslips for 3 to 24 h, followed by fixation of monolayers in 4% formaldehyde for 30 min at room temperature. After 3 washes in PBS, excessive formaldehyde was quenched with 50 mM NH_4Cl for 15 min. Fixed cells were permeabilized with 0.1% Triton X-100 and 0.02% SDS in PBS for 5 min, washed 3 times in PBS (5 min each). Cells were then blocked with 5% FBS in PBS for 30 min, followed by incubation with affinity-purified anti-CpACS antibodies (1:500 dilution in 5% FBS-PBS) for 30 min, three washes with 5% FBS-PBS, incubation with TRITC-conjugated goat anti-rabbit or rabbit anti-chicken IgG (1:400 dilution in 5% FBS-PBS) for 30 min, and three washes with 5% FBS-PBS. After an additional wash

with PBS, coverslips were mounted onto slides with a Prolong Gold Antifade reagent containing 4',6-diamidino-2-phenylindole (DAPI) for counter-staining of nuclei (Molecular Probes/Invitrogen, Grand Island, NY). Cells labeled with fluorescent molecules were examined with an Olympus BX51 research microscope equipped with appropriate filter sets. Images were captured with a Retiga SRV CCD Digital Camera (QImaging, Surry, BC). Fluorescence images were edited with Photoshop CS4. To better visualize the immunofluorescence labeling, images were subjected to adjustments of signal levels and color balance that were uniformly applied to the entire images without local manipulations.

2.2.7 Biochemical assays

All chemicals used in the present study were purchased from Sigma-Aldrich (St. Louis, MO) or as specified. Triacsin C was purchased from Fermentek LTD (Jerusalem, Israel). The activity of CpACS enzymes were determined by monitoring the reduction of CoA concentrations by a 5,5'-Dithio-bis-(2-nitrobenzoate) (DTNB, Ellman's reagent) colorimetric assay. In this assay, free CoA-SH reacted with DTNB to form 5-thionitrobenzoic acids that could be measured at 412 nm (154,155). A typical assay was performed in 200 μL reaction buffer (0.1 M Tris-HCl pH 8.0) containing 10 mM KCl, 10 mM $MgCl_2$, 50 μM CoA-SH, 200 μM ATP and 100 μM fatty acid. A panel of fatty acids with varied chain lengths (C2:0 to C30:0) was individually assays to determine the substrate preferences for CpACS enzymes. The reactions were started with the addition of 1 μg of freshly purified MBP-CpACS fusion proteins. After incubation for 10 min at 32 °C, reactions were stopped by heating sample at 80 °C for 5 min. After samples

cooled down to room temperature, 4 μL of 5 mM DTNB was added into each reaction, followed by 5 min of color development. OD_{412} was measured with a Multiskan Spectrum spectrophotometer (Thermo Scientific, West Palm Beach, FL). The CoA-SH concentration was calculated according to the standard curve using serially diluted CoA-SH solutions.

Enzyme kinetics towards substrates was similarly assayed with varied substrate concentrations (i.e., palmitic acid at 0 – 600 μM and ATP at 0 – 3000 μM, respectively). Guanosine triphosphate (GTP), cytidine triphosphate (CTP) and uridine triphosphate (UTP) were used to replace ATP in the assay to test whether they could serve as alternative energy sources for CpACS enzymes. The inhibitory effects of triacsin C on CpACS enzymes were analyzed under similar reaction conditions, except that 1 to 32 μM of triacsin C was added to reactions. In all experiments, MBP-tag alone was used as control. All assays were carried out in at least duplicate, and at least two independent assays were performed for each experiment.

2.2.8 Drug efficacy against parasite growth in vitro

A quantitative real-time RT-PCR (qRT-PCR) assay was used to evaluate the drug efficacy against *C. parvum* growth in vitro (150,152). Human HCT-8 cells (ATCC # CCL-225) was seeded into 24-well cell culture plates and allowed to grow overnight at 37 °C under an atmosphere of 5% CO_2 in RPMI 1640 medium (Sigma) containing 10% fetal bovine serum (FBS) or until they reached ~80% confluence. Purified *C. parvum* oocysts (less than 3 months old) were added into the cell culture at a parasite:host cell ratio of 1:2 (i.e., 1 x 10^5 oocysts/well), and allowed to infect host cells for 3 h. Parasites

that failed to invade host cells were removed by a medium exchange and tiracsin C were added in the medium (0.2% DMSO). Parasite-infected cells were allowed to grow for additional 41 h. To test the effect of triacsin C on parasite invasion, excystated sporozoites were prepared as described in Section 2.2.1. Sporozoites were incubated with triacsin C at specified concentrations for 30 min at 37 °C, washed with PBS to remove drug, and allowed to invade HCT-8 cells for 3 h. Prior to RNA isolation, monolayers were gently washed 3 times with nuclease-free PBS and lysed in 350 μl of lysis buffer.

Total RNA was isolated from drug treated and untreated cells infected with *C. parvum* using an RNeasy Minikit (Qiagen Inc., Valencia, CA). These RNA samples were also treated with RNase-free DNase (Qiagen) to remove DNA according to the manufacturer's protocol. The quality and purity of RNA were determined using a NanoDrop ND-1000 spectrophotometer at 260/280 nm (Nano-Drop Technologies, Wilmington, DE). A Qiagen one-step RT-PCR QuantiTect SYBR green RT-PCR kit was employed to evaluate the parasite growth. Parasite growth in HCT-8 cells was assayed by detecting the relative levels of parasite 18S rRNA normalized using human 18S rRNA as control as described previously (150,152). Primers used in the assay were listed in Table 2.1. Cytotoxicity of triacsin C on host cells was evaluated by the relative levels of 18S rRNA in uninfected HCT-8 cells and by a 3-(4,5-dimethylthiazol-2-yl)-2,5-diphenyltetrazolium bromide (MTT) assay kit (Sigma) as previously described (23).

2.2.9 Drug efficacy in vivo using a mouse model of acute cryptosporidiosis

The anticryptosporidial activity of triacsin C was assessed in the IL-12 knockout mouse model. The experiments were performed in collaboration with Dr. Jan R. Mead at the Emory University/Atlanta VA Medical Center. Like other mouse models of cryptosporidiosis, this model does not demonstrate frank signs of diarrhea. However, it represents an acute model in that mice have rapidly intensifying parasite loads but then recover by day 14 (101). In this study, *C. parvum* oocysts (IOWA strain) were collected, purified through discontinuous sucrose and cesium chloride gradients and stored as previously described (156). Oocyst inoculation was prepared by washing purified oocysts (stored <6 months) with PBS (pH 7.2) to remove potassium dichromate. Mice (6 - 8 weeks old) were inoculated with 1,000 oocysts and treated by gavage with triacsin C, vehicle control (10% PEG or 1% DMSO), or paromomycin (2 g/kg/d, positive control). Treatment was given once daily for 7 days and mice sacrificed on day 8 (peak infection). At least 10 mice were used for each experimental condition. Parasite burden was assessed by flow cytometry as previously described (157). Briefly, fecal samples were collected from individual mice on 5 and 7 days post-inoculation (dpi) and processed through microscale sucrose gradients in 2.0 ml microcentrifuge tubes. The partially purified stool concentrates containing oocysts were incubated for 30 min at 37 °C with 5 µl of an oocyst wall-specific monoclonal antibody conjugated with fluorescein isothiocyanate (OW50-FITC) and then analyzed by flow cytometry. Absolute counts were calculated from the data files as oocysts per 100 µl of sample suspension (55).

2.2.10 Data analysis and statistics

All biochemical and in vitro drug assays were performed at least in duplicate, and at least two independent assays were performed for each experiment. However, only data derived from single experiments are shown in the figures. In vivo drug testing was performed in two separate experiments. Data were typically analyzed using Microsoft Excel (Office 2011) and GraphPad Prism v5.0f (http://www.graphpad.com). In qRT-PCR analysis for gene expressions and in vitro drug testing, linear and appropriate nonlinear regressions were performed for specified qRT-PCR datasets. Statistical significances were assessed by two-tailed Student's t-test, Mann-Whitney nonparametric test (not assuming Gaussian distributions), and by two-way ANOVA.

2.2.11 Ethics statement

This study was performed in strict accordance with the recommendations in the Guide for the Care and Use of Laboratory Animals of the National Institutes of Health (NIH) under the Animal Welfare Assurance Numbers A4168-01 (Atlanta VA Medical Center) and A3893-01 (Texas A&M University). All animal experiments were performed in accordance with procedures approved by the Institutional Animal Care and Use Committees of Atlanta VA Medical Center (protocol # V001-06) and Texas A&M University (protocol # 2009-21).

2.3 Results

2.3.1 CpACS enzymes belong to the long-chain ACS subfamily

ACS enzymes can be divided into four major subfamilies based on the chain length of their preferred acyl groups: short-chain (C2 - C4) (SC)-ACS, medium-chain (C4 - C12) (MC)-ACS, long-chain (C12 - C20) (LC)-ACS, and very long-chain (C18-C26) (VLC)-ACS (134,158). The number of LC-ACSs varies among different organisms (e.g., at least 9 in *Arabidopsis thaliana*, 11 in *Plasmodium falciparum* and 5 in humans) (148,158,159). Each of the three sequenced *Cryptosporidium* genomes (i.e., *C. parvum*, *C. homins* and *C. muris*) contains three LC-ACS genes. Our sequence analysis indicated that LC-ACSs are closely related to VLC-ACSs. Phylogenetic trees inferred from chromalveolate orthologs by ML and BI methods divided the LC- and VLC-ACS proteins into 4 major clusters (Figure 2.1): clusters I and II with top hits to eukaryotic-type LC-ACS domains in the NCBI conserved domain database (e.g., LC-ACS-euk [cd05927]); cluster III with Firefly Luc-like (cd05911) and uncharacterized FACL-like-2 (cd05917) domains; and cluster IV with VLC-ACS (cd05907) and bubblegum VLC-ACS (cd05933). Sequences from stramenopiles and ciliates were present in all 4 clusters, while those from a dinoflagellate (*Perkinsus*) and apicomplexans were mainly present in clusters I and II, except of *Toxoplasma* and *Neospora. Toxoplasma* and *Neospora* both had two ACS sequences in cluster IV.

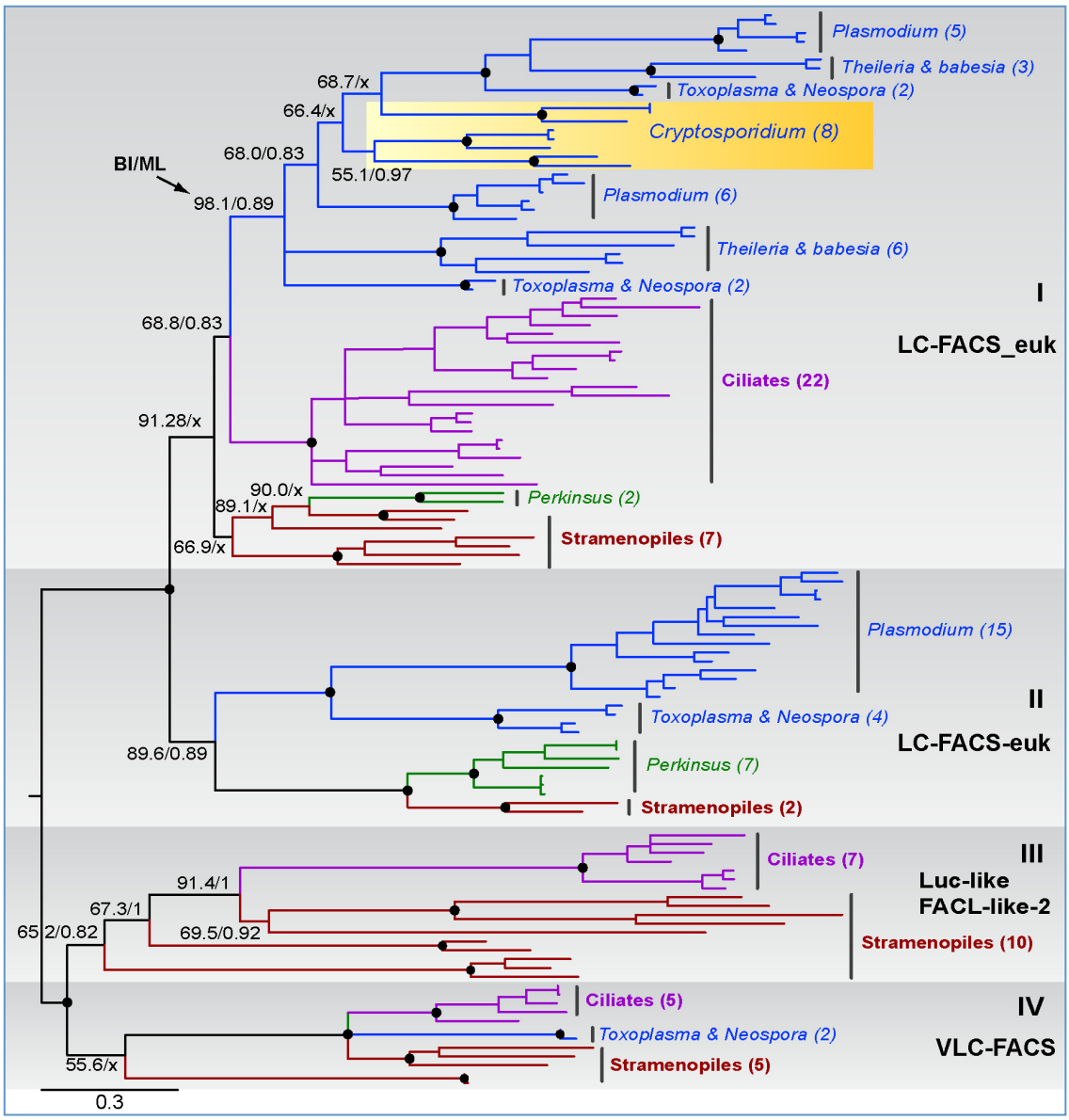

Figure 2.1 Phylogenetic tree inferred from ACS proteins among chromalveolates using Bayesian inference (BI) and maximum likelihood (ML) methods. Numbers at the nodes indicate posterior probability and bootstrapping proportion supporting values obtained in BI and ML analyses. Numbers of sequences contained in specified clusters are indicated in parentheses after the taxonomic names.

These observations suggest that: 1) there was an ancient split between LC- and VLC-ACS genes that predated the split between alveolates and stramenopiles; 2) VLC-ACS genes were lost in most apicomplexans and in at least one dinoflagellate (*Perkinsus*), but were retained in some coccidia (e.g., *Toxoplasma* and *Neospora*); and 3) gene expansions occurred within each group, particularly among the LC-ACS genes in clusters I and II.

All *Cryptosporidium* ACS proteins were predicated to be LC-ACS enzymes in cluster I, which was confirmed by biochemical analysis as described below. The three CpACS proteins contained two conserved domains: the AMP/ATP-binding motif (TSGTTGxPK) and the fatty acyl-CoA synthetase signature motif (TGDIxxxxxxGxxxIxDRxK) (Figure 2.2A). The AMP/ATP-binding sites are highly conserved not only in the ACS family, but also in many other ATP-dependent AMP-binding enzymes for adenylate formation (144,160). Signal peptides (SP) were absent in both the CpACS1 and CpACS2 proteins. However, SignalP analysis indicated the presence of an N-terminal signal peptide for secretion (S-score: 0.97) with a predicted cleavage site between amino acid positions 22 and 23 of CpACS3 (Figure 2.2B).

2.3.2 CpACS genes were differentially expressed and their proteins were localized to different subcellular structures

Having established that the *CpACS* genes likely encode long-chain ACS enzymes, we wanted to confirm the expression and localization of these enzymes. This information could provide additional insight into the biological function of these

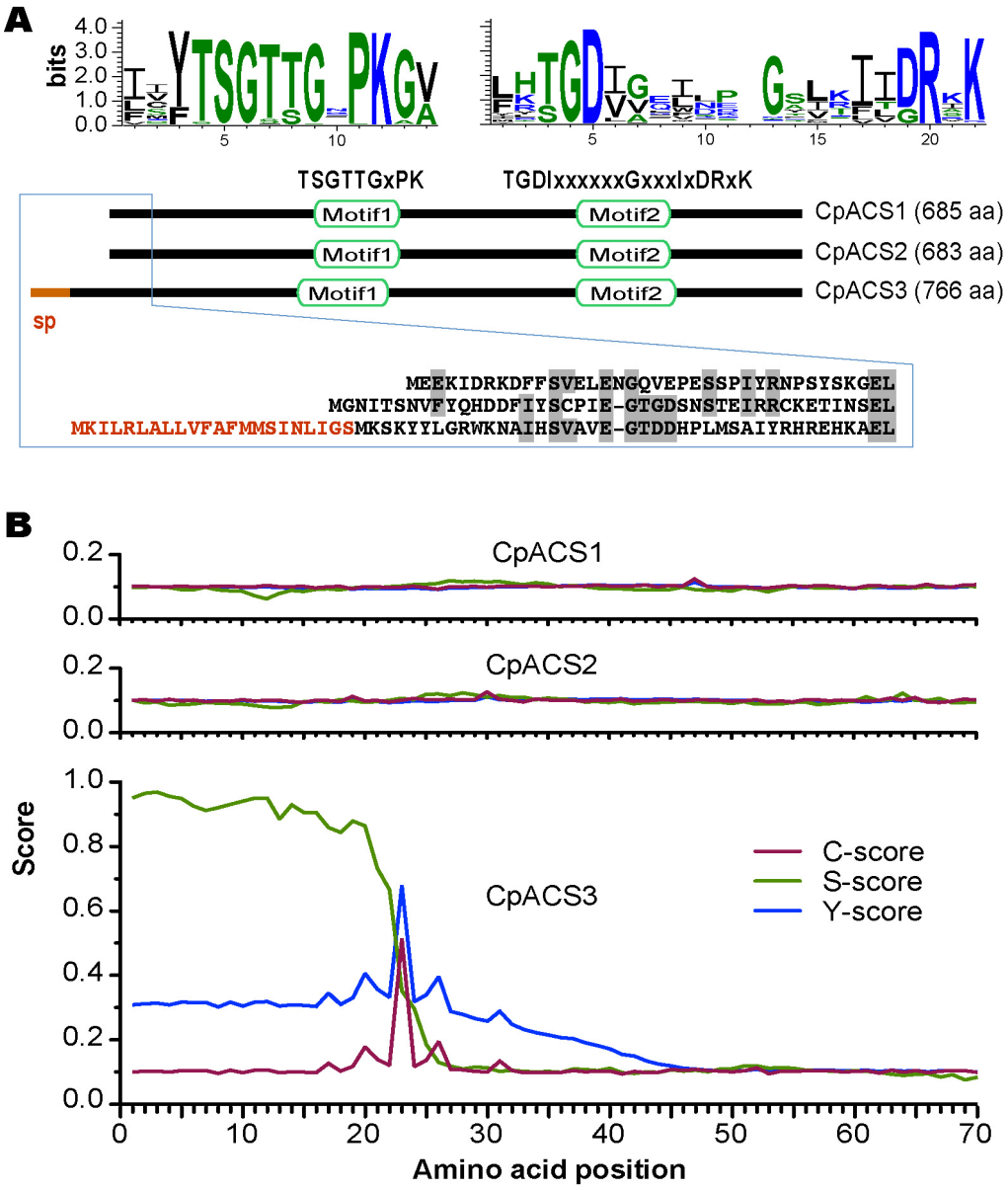

Figure 2.2 Structures and domains for CpACS1, CpACS2 and CpACS3 proteins. A) Domain organization and sequence logos of amino acids conserved among chromaveolates; B) Prediction of N-terminal signal peptide (sp) for secretion in CpACS3 by SignalP algorithm, in which S-score predicts signal peptide, while C-score and Y-score predict cleavage site.

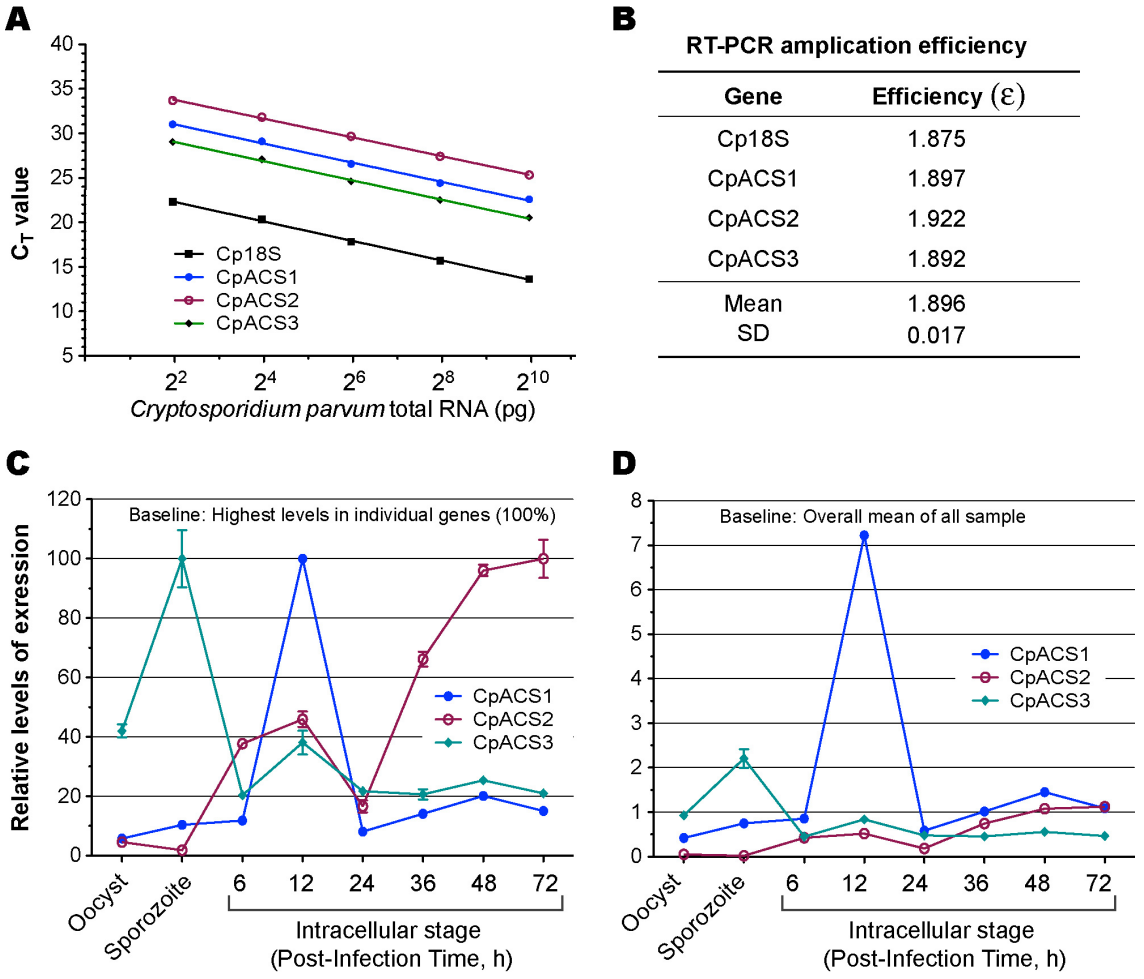

Figure 2.3 Differential expression of the 3 CpACS genes in *C. parvum* at different life cycle stages as determined by qRT-PCR. A) Standard curves showing linear relationship between detection threshold cycles (C_T values) and the levels of CpACS transcripts using serially diluted, pooled total RNA isolated from infected HCT-8 cells. Cp18S rRNA was used as control for normalization; B) PCR amplification efficiencies of Cp18S rRNA and CpACS transcripts derived from standard curves; C) Normalized levels of three CpACS transcripts in different life cycle stages in relative to the highest level for each gene (i.e., comparison between different developmental stages, but not between different genes); D) Normalized levels of three CpACS transcripts in relative to the overall mean of all three genes in all developmental stages.

enzymes. We examined the levels of CpACS transcripts and protein localizations in various parasite developmental stages by qRT-PCR and immunofluorescence microscopy, respectively. Because the PCR amplification efficiencies for all three genes and Cp18S rRNA were nearly identical (i.e., $\boldsymbol{\varepsilon} = 1.896 \pm 0.017$) (Figure 2.3A and 2.3B), we were able to use the $\Delta\Delta C_T$ method to directly compare the relative levels of expressions of between three CpACS genes in all samples against the overall mean (Figure 2.3D). We also compared the mRNA levels of a specified gene in various samples (Figure 2.3C). Real-time qRT-PCR based analysis revealed that CpACS genes were differentially expressed at different parasite developmental stages (Figures 2.3C and 2.3D). More specifically, the *CpACS1* and *CpACS2* genes were expressed at much higher levels in the early and later intracellular developmental stages, respectively. On the other hand, the *CpACS3* gene had much higher levels of expression in oocysts and sporozoites (Figure 2.3C). These observations suggest that the three CpACS enzymes might play different roles during the parasite development.

This notion was also supported by immunofluorescence staining using affinity-purified polyclonal antibodies against the three CpACS proteins (Figures 2.4, 2.5 and 2.6). CpACS1 was highly concentrated in the anterior region of free sporozoites and merozoites (Figure 2.4), which corresponding to the region containing apicomplexan-specific secretory organelles micronemes and rhoptries. CpACS1 protein was briefly retained in the anterior region after sporozoites and merozoites entered host cells (i.e., single-nuclear early stage of merogony), fully dissolved in the mid-stage of

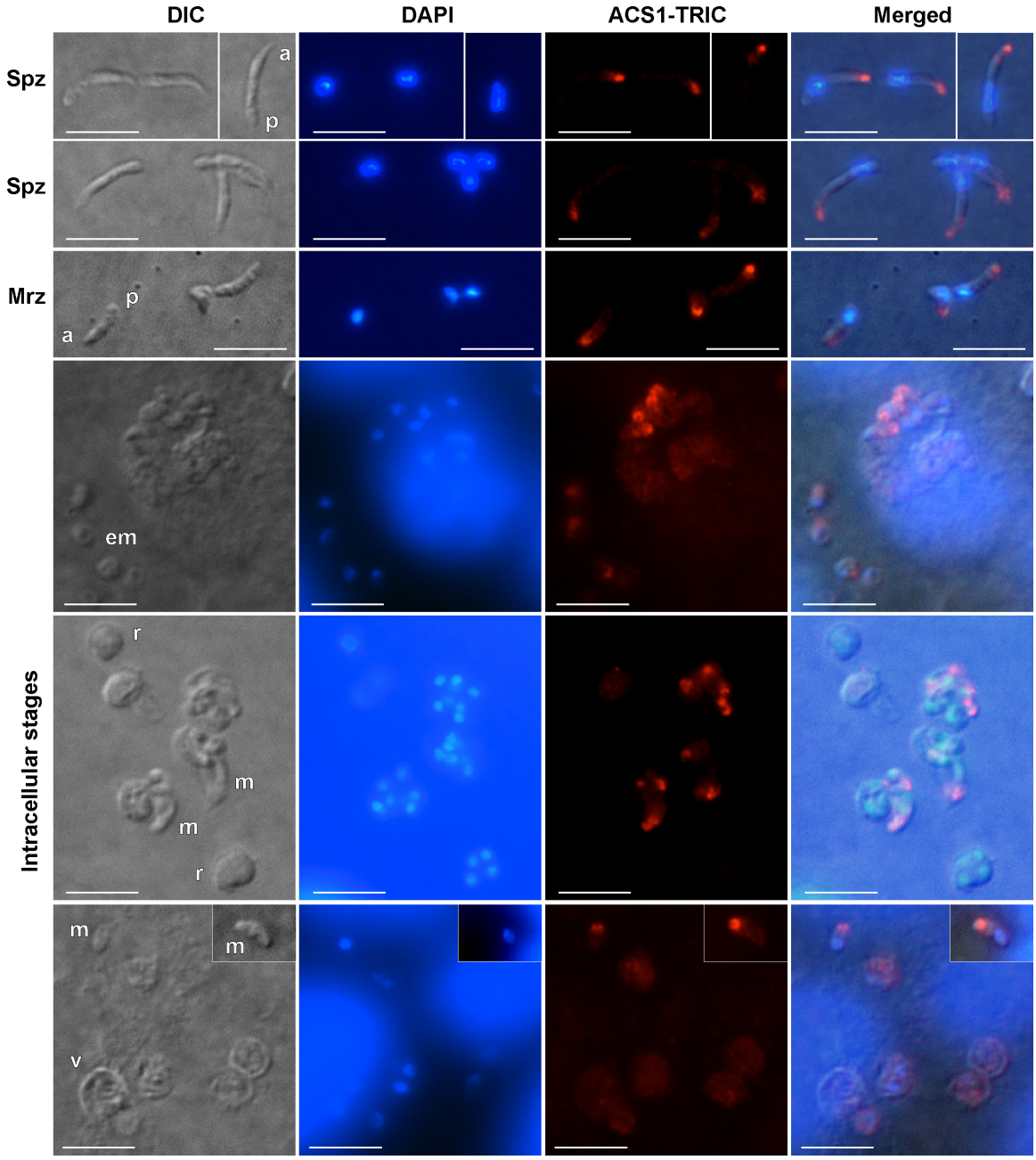

Figure 2.4 Immunofluorescence labeling of CpACS1 protein in *C. parvum* sporozoites (Spz), merozoites (Mrz) and intracellular developmental stages. Abbreviations: a, anterior region of sporozoites or merozoites; p, posterior region of sporozoites or merozoites; em, early stage meronts; m, meronts; r, merozoites; v, parasitophorous vacuole membrane.

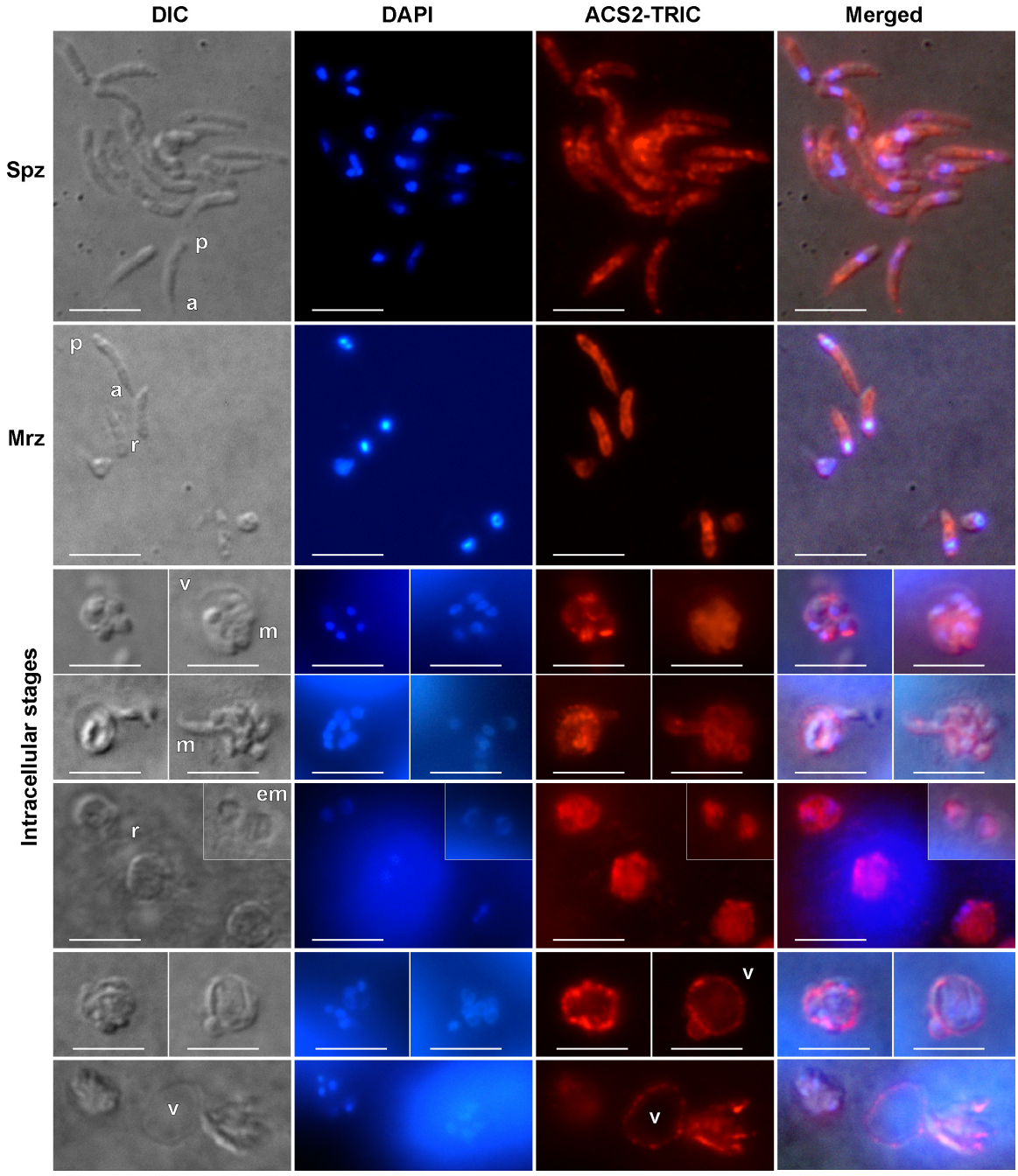

Figure 2.5 Immunofluorescence labeling of CpACS2 protein in *C. parvum* sporozoites (Spz), merozoites (Mrz) and intracellular developmental stages. See Figure 2.4 legend for abbreviations.

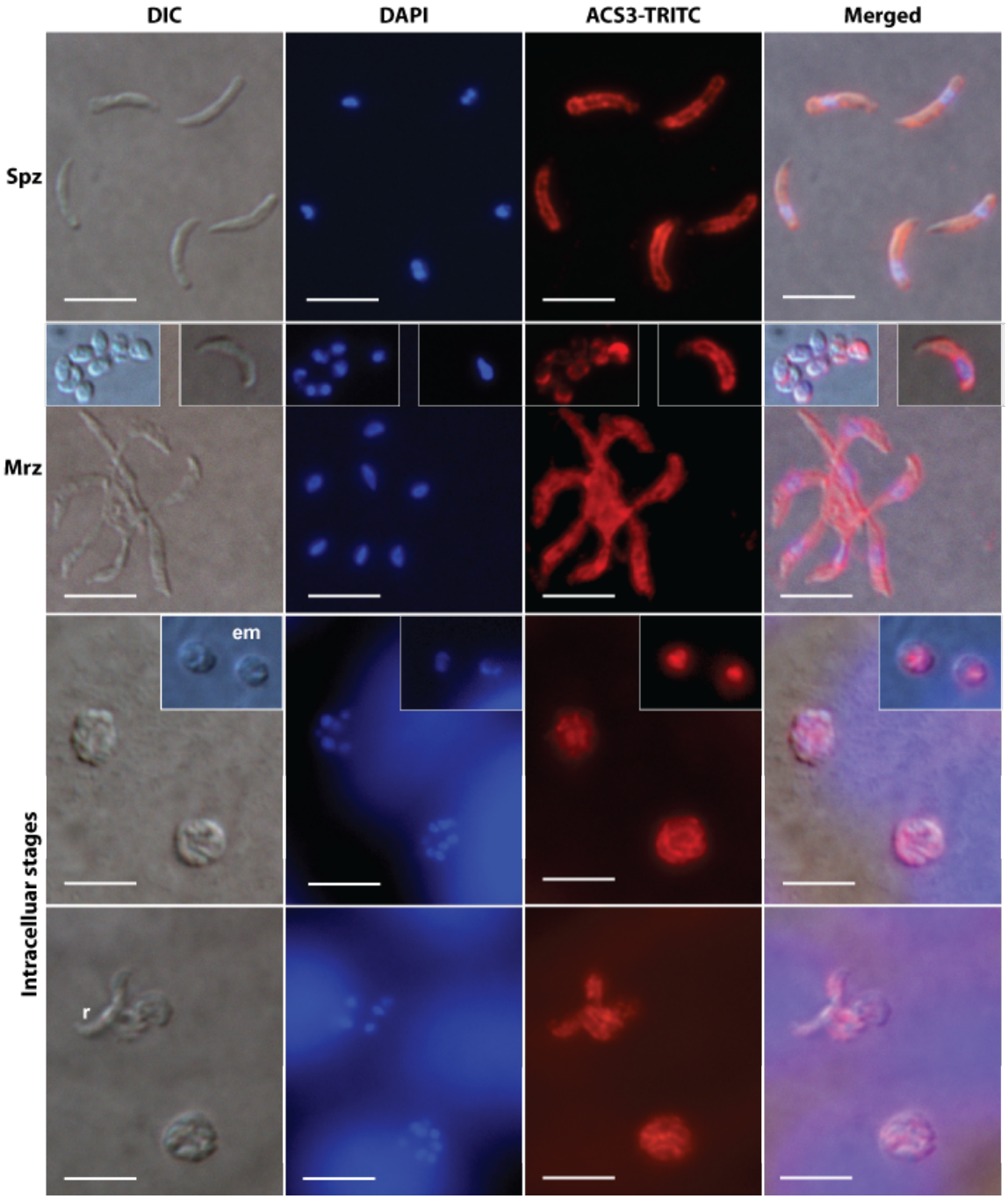

Figure 2.6 Immunofluorescence labeling of CpACS3 protein in *C. parvum* sporozoites (Spz), merozoites (Mrz) and intracellular developmental stages. See Figure 2.4 legend for abbreviations.

multi-nuclear meronts with no or weak fluorescence signal, and then reappeared in the anterior region of intracellular merozoites in the late stage of merogony (Figure 2.4). Additionally, weak signals were also observed in parasitophorous vacuole membrane (PVM). Based on these observations, we speculate that CpACS1 is probably stored in rhoptries and/or micronemes, and mainly participates in the activation of fatty acids that may be required in the early stage of intracellular development.

On the other hand, CpACS2 protein was highly concentrated in the cytoplasmic membranes in virtually all stages of *C. parvum*, including free sporozoites and merozoites, and intracellular parasites at various developmental stages (Figure 2.5). CpACS2 protein was also present in the PVM. However, it was highly concentrated in certain region with focal points slightly different from those of intracellular merozoites towards host cells, similar to a previously reported ATP-binding cassette (ABC) transporter (161), suggesting that this enzyme might be more concentrated at the parasite-host cell interface than in PVM. These observations suggest that CpACS2 may play a general house-keeping role in the parasite, and may be involved in the scavenging of fatty acids from host cells.

CpACS3 distributed in a similar pattern as CpACS2 in the parasite cells, i.e., highly concentrated on the cytoplasmic membranes in sporozoites, merozoites and intracellular parasites (Figure 2.6). However, unlike CpACS2, there was no or little CpACS3 on the PVM during the intracellular developmental stages, suggesting that CpACS3 may mainly function in the parasite cells, but less likely be involved in the uptake of fatty acids from host cells across the PVM or feeder organelle.

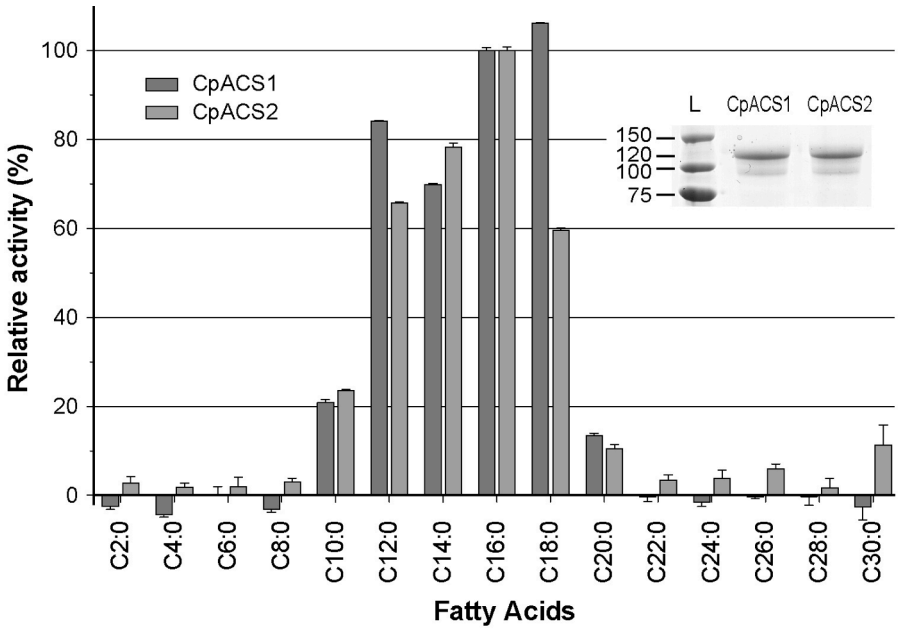

Figure 2.7 Activation of long chain fatty acids by *C. parvum* ACSs. Substrate preferences of recombinant CpACS1 and CpACS2 proteins towards variable carbon chain lengths of saturated fatty acids as determined by DTNB assay. Activities are expressed in relative to C16 palmitic acid.

2.3.3 CpACS1 and CpACS2 activate long-chain fatty acids

To test whether or not the CpACSs represent bona-fide fatty acid activating enzymes, we attempted to clone and express these proteins as MBP-fusion proteins in bacteria and examined their activity against saturated fatty acids. All three CpACS genes could be amplified by PCR, cloned into the pCR2.1-TOPO cloning vector, and subcloned into the expression vector pMAL-c2x. However, only CpACS1 and CpACS2 have been successfully expressed as recombinant proteins (Figure 2.7, inset). Numerous

attempts to express recombinant CpACS3 were unsuccessful, including the use of different expression conditions and vectors. Therefore, biochemical analyses reported here were focused on the recombinant CpACS1 and CpACS2 to gain knowledge of biochemical features representing CpACS enzymes in general.

Classic ACS assays use radioactive substrates coupled with isopropanol and/or heptane extractions [e.g. (162,163)]. Here we adapted a colorimetric assay using 5,5'-Dithio-bis-(2nitrobenzoate) (DTNB, Ellman's reagent) to assess enzyme kinetics and inhibitor effects by measuring the reduction of thiol-groups of free CoA-SH in the reactions (164). This method is more user-friendly, safer, and suitable for adaptation to high-throughput screening. Both CpACS1 and CpACS2 displayed a clear preference towards 12- to 18-carbon fatty acids and lower activities toward C10:0 and C20:0 (Figure 2.7). These two enzymes had no or little activity on saturated fatty acids that are less than 10 carbons or greater than 20 carbons in length, except for CpACS2 which displayed low activity towards some VLC fatty acids. The data agree with the functional prediction based on phylogenetic reconstructions.

CpACS1 and CpACS2 followed Michaelis-Menten kinetics towards C16:0 (palmitic acid) and ATP with K_m values in the lower μM and nM levels, respectively (Table 2.2 and Figures 2.8A and 2.8B). The two enzymes were Mg^{2+}-dependent, and their activities peaked at ~1 mM Mg^{2+} concentrations (Figure 2.8C). Both enzymes could only utilize ATP as their energy source, as no activities were observed when GTP, CTP and UTP were used in the reactions (Figure 2.8D), which was similar to the *P.*

falciparum ACS1 and the ACL-domain in the *C. parvum* polyketide synthase (CpPKS1) (162,163).

Table 2.2 CpACS1 and CpACS2 enzyme kinetics towards substrates and inhibitor

Substrate or inhibitor	**Parameter**	**CpACS1**	**CpACS2**
Palmitic acid	$\boldsymbol{K_m}$ (μM)	38.30	7.21
Palmitic acid	$\boldsymbol{V_{max}}$ (mmol/mg/min)	0.60	0.78
ATP	$\boldsymbol{K_m}$ (μM)	0.26	0.17
ATP	$\boldsymbol{V_{max}}$ (mmol/mg/min)	0.81	1.62
Triacsin C	$\mathbf{IC_{50}}$ (μM)	3.70	2.32
Triacsin C	$\boldsymbol{K_i}$ (μM)	0.60	0.11

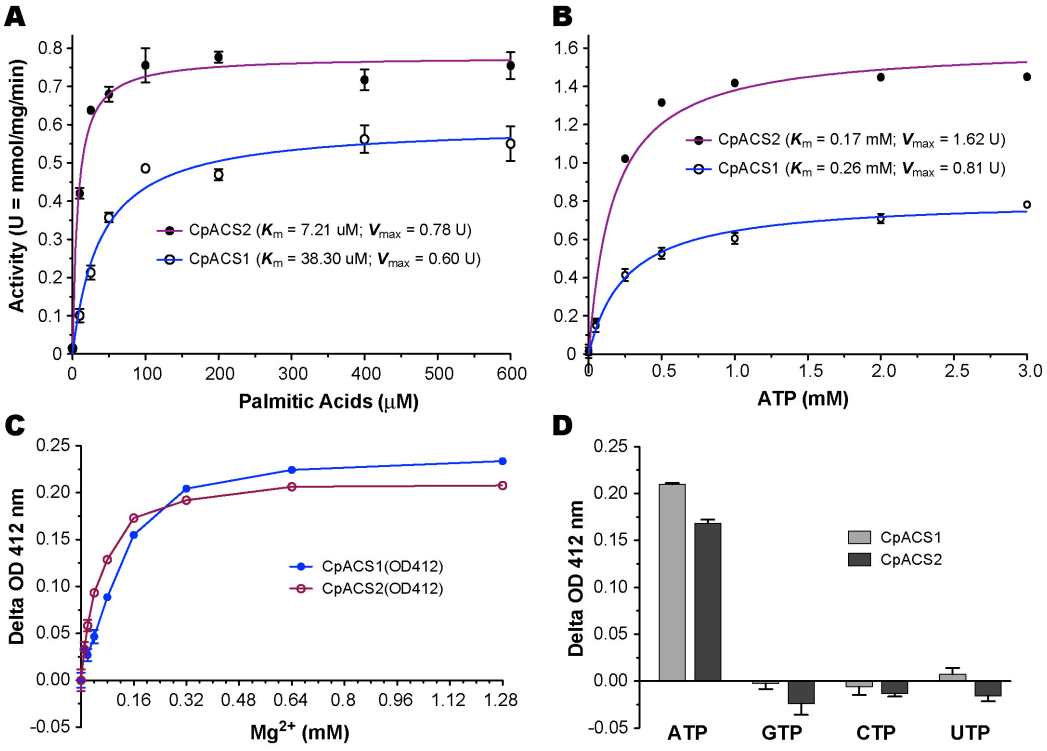

Figure 2.8 Biochemical features of CpACS1 and CpACS2 as determined using recombinant proteins. A) Enzyme kinetics towards palmitic acid; B) Enzyme kinetics using ATP; C) Dose-dependent activity using Mg^{2+}; D) Enzyme activities using different nucleoside triphosphates (NTPs).

2.3.4 Triacsin C inhibited CpACS enzyme activities and was highly effective against C. parvum growth both in vitro and in vivo

To assess whether or not CpACS enzymes are amenable to inhibition by small molecules, we examined enzyme activities in the presence of triacsin C (CAS # 76896-80-5; synonym: 2,4,7-undecatrienal nitrosohydrazone) that is a fungal metabolite

originally isolated from *Streptomyces aureofaciens* and identified as a vasodilator (165,166). It resembles a polyunsaturated fatty acid (see Figure 2.9B inset) and can differentially inhibit various LC-ACSs (167-172). For example, in humans, it can inhibit LC-ACSs, but has little effect on SC-ACSs or mitochondrial MC-ACSs (170). In rats, this compound was effective on ACSL1, ACSL3 and ACSL4 at low μM levels, but was not effective against ACSL5 and ACSL6 (171,172). In the present study, we observed that triacsin C could inhibit CpACS1 and CpACS2 enzyme activities with IC_{50} values at 3.70 μM and 2.32 μM (Table 2.2 and Figure 2.9A), corresponding to K_i values at 595 nM and 106 nM, respectively, as calculated using a competitive inhibition model (173).

Given that triacsin C displayed significant inhibition of the CpACS enzymes in vitro, we wished to determine if this compound was effective at inhibiting parasite growth. Triacsin C displayed strong efficacy against the growth of *C. parvum* cultured with HCT-8 cells at nM levels (i.e., $\mathbf{IC_{50}}$ = 136 nM) (Figure 2.9B), although a short 30-min treatment on sporozoites did not affect parasite invasion (Figure 2.9C). There were no significant effects of triacsin C on the HCT-8 host cells based on the Hs18S rRNA levels (Figure 2.9D), and MTT assay suggested a moderate decrease in host cell metabolism when this inhibitor was used at 1 μM or higher for 2 days (Figure 2.9E).

The promising results of triacsin C against both CpACS enzyme activity and parasite growth in vitro motivated us to examine how triacsin C would affect the pathogenesis of disease in a mouse model of acute cryptosporidiosis. In vivo drug testing using an IL-12 knockout mouse model of acute cryptosporidial infection revealed that

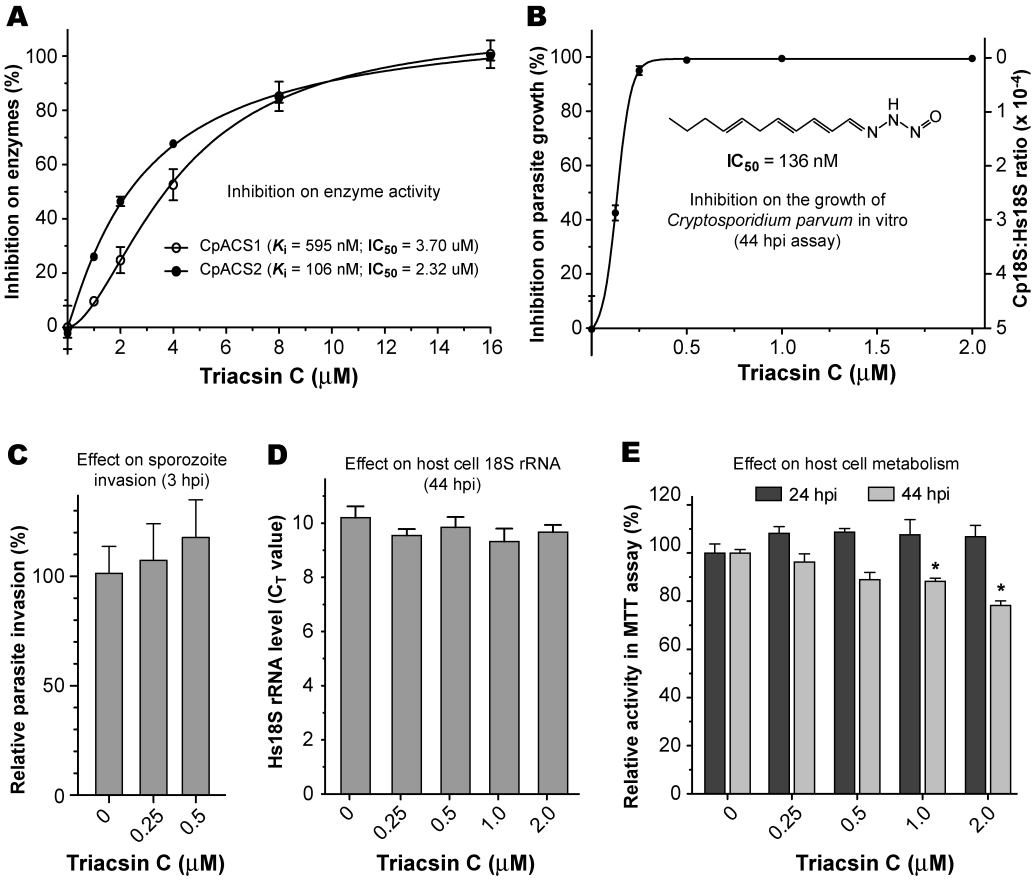

Figure 2.9 Inhibition of enzyme activity and parasite growth in vitro. A) Inhibition of CpACS1 and CpACS2 enzyme activities by triacsin C; B) Efficacy of triacsin C on the growth of *C. parvum* cultured in vitro with HCT-8 cells using a qRT-PCR assay at 44h post-infection (hpi); C) Relative level of invasion by sporozoites receiving 30-min treatment of triacsin C determined at 3 h post infection (hpi); D) Effect of triacsin C treatment on the Hs18S rRNA levels in the uninfected HCT-8 cells; E) Effect of triacsin C on uninfected HCT-8 cell metabolism by an MTT assay. Asterisks indicate groups with statistically significant differences when compared untreated controls ($p < 0.05$).

triacsin C could effectively inhibit the parasite growth at therapeutic levels. At a dose of 8 mg/kg/d, triacsin C reduced *C. parvum* oocyst production in feces by 62.50% and 54.73% on 5 and 7 dpi, respectively; while at 15 mg/kg/d the reductions reached 78.91% and 88.11% on 5 and 7 dpi, respectively (Figure 2.10A). Both Student's *t*-test and nonparametric test indicated the reductions were significant in all treated groups except for the 8 mg/kg/d group. Two-way ANOVA also showed significant differences in percent inhibitions between the two doses of triacsin C treatments ($p = 0.020$), but not between 5 and 7 dpi ($p = 0.316$) (Figure 2.10A). Additionally, gross histology of IL-12 knockout mice administered 8 or 15 mg/kg/d doses of triacsin C revealed no observable pathology in the major organs (data not shown). Moreover, triacsin C treatments at the two doses resulted in a general improvement in weight gain in mice infected with *C. parvum*, although the improvement was not statistically significant by Student's *t*-test or Mann-Whitney test (Figure 2.10B).

The observed therapeutic index of triacsin C against cryptosporidial infection in mice was more than 10 times better than nitazoxanide (the only FDA-approved drug to treat human cryptosporidiosis) and paromomycin (a "golden standard" anti-cryptosporidial control drug), as these two classic anti-cryptosporidial drugs could only effectively inhibit cryptosporidial infections in various animal models at doses between 0.2 – 2 g/kg/d (Figure 2.10A) [also see review (174)].

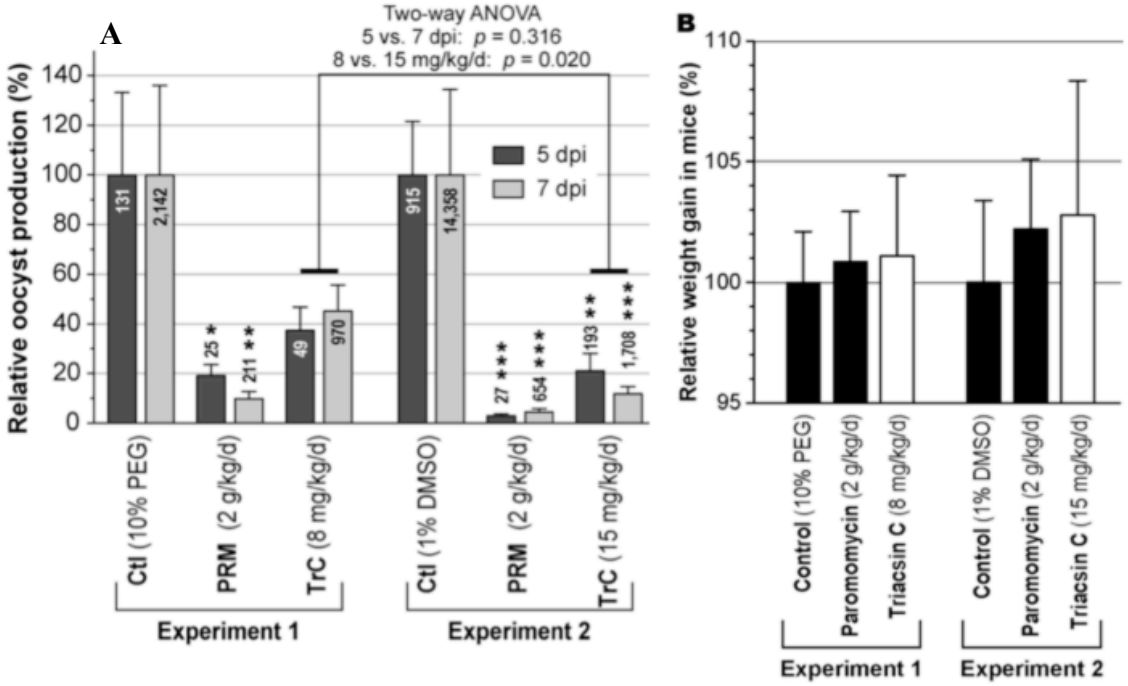

Figure 2.10 Efficacy of triacsin C on cryptosporidial infection in IL-12 knockout mice. A) Relative production of *C. parvum* oocysts on 5 and 7 days post-infection (dpi). Numbers in or above the bars indicate average oocyst counts (per 100µL) in each experimental group. Asterisks indicate statistically significant difference by a nonparametric Mann-Whitney test when compared with controls (* = $p < 0.05$; ** = $p < 0.01$; *** = $p < 0.001$). Student's *t*-test produced the same result, albeit with smaller *p* values (all < 0.05); B) Relative weight gains in mice on day 7 pi. No significant difference in mice weight gain was showed between different treatment within and between two experiments.

Nitazoxanide and paromomycin are known for their low toxicity to humans and animals (e.g., oral **LD_{50}** values for acute toxicity in mice at 1.35 and 23.5 g/kg/d, based on the Registry of Toxic Effects of Chemical Substances database). Although toxicity of triacsin C in mice remains to be determined, this compound was not toxic to mice at the low mg/kg/d levels used here and in other studies (175,176).

2.4 Discussion

We identified three long chain fatty acyl-CoA synthetase (LC-ACS) genes in the *C. parvum* genome that were differentially expressed during the complex parasite life cycle. Their protein sequences were 98% (ACS3) to 100% (ACS1 and ACS2) identical to the orthologs in *C. hominis*, or 73% to 76% identical to those from *C. muris*. CpACS1 and CpACS2 were successfully expressed as MBP-fusion proteins. Even though different strategies have been explored to express CpACS3 in *E. coli*, we were still unable to get induced CpACS3 protein. It might due to potential cytotoxicity of this protein to *E. coli*, which likes *P. falciparum* ACS1 (163). However, our biochemical analysis on CpACS1 and CpACS2 provide sufficient insights on the biochemical features of this family of enzymes in *C. parvum*. The DTNB-based colorimetric assay not only permits the measurements of enzyme activity and the effect of inhibitors, it can also be easily adapted for high-throughput screening of drugs against ACS.

Despite that LC-ACS enzymes are essential in fatty acid metabolism and present in multiple forms in various apicomplexans, little is known on their biochemical features. In fact, only one earlier study had assayed the ACS activity in crude extract of

P. knowlesi-infected simian erythrocytes (177), and a relatively simple biochemical analysis was performed specifically on a single *P. falciparum* ACS (i.e., PfACS1) protein (163). In *C. parvum*, one of the three ACS genes (corresponding to *CpACS3*) was previously identified by screening an expression library with a monoclonal antibody (178), but no biochemical analysis was performed. The lack of functional study on apicomplexan ACSs might be in part due to the technical difficulties in expressing and/or obtaining enzymatically active recombinant proteins as noted in expressing CpACS3 (this study) and PfACS1 (163). Therefore, our observation that recombinant CpACS1 and CpACS2 proteins retain activity for only a very short time and need to be assayed immediately after purification is a critical one, and should be kept in mind when studying other recombinant apicomplexan ACS enzymes. On the other hand, addition of 10 mM of ATP in protein stocking buffer can improve CpACS stability as shown in stocking of *E. coli* FadR (ACS) (179). Although the ATP in stocking buffer will affect the analysis of biochemical features, high-throughput screening of drugs against CpACSs will greatly benefit from the stability improvement of CpACS proteins.

The most significant observation is the excellent efficacy of ACS inhibitor triacsin C against cryptosporidial infection in mice. Because of the lack of completely effective drugs for cryptosporidiosis in humans and animals, particularly in AIDS patients, great efforts have been devoted to the drug discovery against this parasite. Drug screenings have, in fact, identified many compounds highly effective against the growth of *C. parvum* in vitro, but most (if not all), including nitazoxanide and paromomycin, failed to achieve comparable efficacies when tested in animals (174,180). The present

study shows that triacsin C effectively inhibited specific drug targets CpACS1 and CpACS2, displayed excellent therapeutic indexes against the growth of *C. parvum* in vitro (i.e., IC_{50} = 136 nM), and could reduce *C. parvum* oocyst production in mice by ~50% to 88% at pharmaceutically achievable levels (i.e., 8-15 mg/kg/d).

It is known that triacsin C may also inhibit LC-ACS enzymes in humans and animals, thus affecting certain aspects of lipid metabolism. For example, treatment of human hepatocytes with triacsin C reduced the formation of lipid droplets (181), while in human fibroblast cells, it could block de novo synthesis of glycerolipids and cholesterol esters (182). However, triacsin C did not affect the recycling of fatty acids into phospholipid, which not only suggests the presence of functionally separate pools of acyl-CoA, but also explains why no apparent toxicity occurred in the animals used here and previous studies (182). Although triacsin C has not been tested or therapeutically used in humans, several studies in animals have shown the benefits of triacsin C treatment. For example, in vitro and in vivo experiments in chickens have shown that triacsin C could rescue palmitic acid-induced cytotoxicity of follicle granulosa cells in fuel-overloaded broiler hens (183). In mice, triacsin C displayed activities to control cancer growth and enhance the efficacy of etoposide at a non-toxic dose (4 mg/kg/d) (175), and anti-atherosclerotic activity when administrated at a dose of 10 mg/kg/d (184). These observations suggested that, although pharmacokinetics and toxicity tests are needed to further evaluate the safety, triacsin C is generally safe in animals when administrated at low mg/kg/d doses, and that its potential as a new anti-cryptosporidial drug should be explored. In fact, triacsin C is also an effective inhibitor against the acyl-

CoA-[ACP]-ligase domains in the unique, multi-functional type I fatty acid synthase (FAS1) and polyketide synthase (PKS1) in *C. parvum* (162). Therefore, triacsin C has the potential to hit multiple targets and to block both the fatty acid activation by discrete ACSs, as well as elongation of fatty acids by FAS1 and PKS1.

Finally, whether triacsin C could be truly developed into a new anti-cryptosporidial drug may require a serial pharmacokinetic, preclinical and clinical tests, the present study strongly supports that the discrete ACSs (and ACL domains in FAS1 and PKS1) can serve as novel drug targets. New triacsin C analogs can be synthesized and new classes of anti-ACS compounds may be identified by drug screening for developing more selective and safe anti-cryptosporidial drugs.

3 SUMMARY AND CONCLUSION

C. parvum is a unicellular zoonotic pathogen that can cause severe watery diarrhea in both humans and animals (185). Individuals with immune system dysfunction, such as recipients of chemotherapy and AIDS patients are at high risk because *C. parvum* can cause a severe and sometimes fatal diarrhea to them. More significantly, *Cryptosporidium* is emerging as one of the four top diarrheal pathogens in children <2 years old in developing countries (69). Although the introduction of HAART has tremendously decreased the cryptosporidiosis on AIDS patients in developed countries, HAARP is not widely available in developing countries. Moreover, cryptosporidiosis is not always associated with AIDS in children, and HAARP may not eligible for non-HIV infected children. In the United States however, FDA approved treatments remain unavailable to treat this opportunistic infection in patients with AIDS, whereas only nitazoxanide is approved for use in immunocompetent individuals. Therefore, there is an urgent need for new drugs, particularly those that can be safely used in children and immunocompromised persons.

In the present study, we explored the parasite fatty acyl-coenzyme A synthetase (ACS) as a novel drug target. ACS catalyzes the thioesterification between free fatty acids and CoA to form fatty acyl-CoAs. Fatty acyl-CoA is the active form of fatty acids, which will enter various metabolic pathways, such as β-oxidation, membrane lipid synthesis. Because fatty acids have to be activated by ACS to form acyl-CoA thioesters

before they involve in different biological pathways, ACS is essential in virtually all organisms.

The *C. parvum* genome encodes three potential ACSs, and they all cotain AMP/ATP binding domain and fatty acyl-CoA synthetase signature domain that are functional essential to ACS family enzyme. Phylogenetic tree inferred from ACS proteins among chromaleolates showed that all CpACSs proteins were predicted to be long chain ACS. Our biochemical result also confirmed that CpACS1 and CpACS2 both displayed a clear preference towards long chain fatty acids (C12- to C18- carbon). In vitro HCT-8 cells infection assays showed that three CpACSs were expressed in all parasite life cycle stages, but differed in their transcription profiles. For example, CpACS1 was highly expressed during first generation merogonic development, CpACS2 during second generation of merogony, and CpACS3 in oocyst and sporozoites stages. The different transcription patterns of CpACSs suggest that they might play different roles during the parasite development.

Indirect immunoflouresence labeling showed that CpACS1 protein was mainly located in the anterior region of the free sporozoites and merozoites, and disappeared in the middle multinuclear meront stage. CpACS2 protein was highly concentrated in the cytoplasmic membranes in virtually all stages of *C. parvum*, and also in PVM. CpACS3 showed similar localization pattern as CpACS2 in parasites, but not present in PVM. The different subcellular localizations of CpACSs further support the notion that they play different role during parasite development.

We observed that Triacsin C, one typical ACS inhibitor, could inhibit CpACS1 and CpACS2 enzyme activities at low μM levels. In vitro assay on *C. parvum* infected HCT-8 cells, triacsin C displayed strong efficacy against the growth of *C. parvum* at low nM levels. Furthermore, in vivo assay performed on IL-12 knockout mice model of acute cryptosporidiosis demonstrated that the effective dose of triacsin C against *C. parvum* infection was more than 10 times better than paromomycin and nitazoxanide.

In summary, we have provided compelling evidence that fatty acid metabolism in *C. parvum* is essential and amenable to inhibition. The three CpACSs showed different transcription patterns and subcellular localizations. Both CpACS1 and CpACS2 prefer to use long chain fatty acids, and their enzyme activities can be inhibited by triacsin C, which is a long chain fatty acids analog. Triacsin C was highly effective against *C. parvum* growth in vitro (IC_{50} = 136 nM). Most importantly, triacsin C effectively reduced parasite oocyst production up to 88.1% with no apparent toxicity when administered to *Cryptosporidium*-infected interleukin 12 knockout mice at 8–15 mg/kg/d for 1 week. The findings of this study not only validated CpACSs as pharmacological targets, but also indicated that triacsin C and analogues can be explored as potential new therapeutics against the virtually untreatable cryptosporidial infection in immunocompromised patients.

REFERENCES

1. Tyzzer, E. E. (1908) A sporozoan found in the peptic glands of the common mouse. *P Soc Exp Biol Med* **5**, 12-13

2. Tyzzer, E. E. (1912) *Cryptosporidium parvum* (sp. nov.),a coccidium found in the small intestine of the common mouse. *Arch. Protistenkd.* **26**, 394-412

3. Nime, F. A., Burek, J. D., Page, D. L., Holscher, M. A., and Yardley, J. H. (1976) Acute Enterocolitis in a Human Being Infected with Protozoan Cryptosporidium. *Gastroenterology* **70**, 592-598

4. Meisel, J. L., Perera, D. R., Meligro, C., and Rubin, C. E. (1976) Overwhelming Watery Diarrhea Associated with a *Cryptosporidium* in an Immunosuppressed Patient. *Gastroenterology* **70**, 1156-1160

5. Bird, R. G., and Smith, M. D. (1980) Cryptosporidiosis in man: parasite life cycle and fine structural pathology. *The Journal of Pathology* **132**, 217-233

6. Navin, T. R., and Juranek, D. D. (1984) Cryptosporidiosis: clinical, epidemiologic, and parasitologic review. *Reviews of Infectious Diseases* **6**, 313-327

7. Hayes, E. B., Matte, T. D., O'Brien, T. R., McKinley, T. W., Logsdon, G. S., Rose, J. B., Ungar, B. L., Word, D. M., Pinsky, P. F., Cummings, M. L., and et al. (1989) Large community outbreak of cryptosporidiosis due to contamination of a filtered public water supply. *The New England Journal of Medicine* **320**, 1372-1376

8. Corso, P. S., Kramer, M. H., Blair, K. A., Addiss, D. G., Davis, J. P., and Haddix, A. C. (2003) Cost of illness in the 1993 waterborne *Cryptosporidium* outbreak, Milwaukee, Wisconsin. *Emerging Infectious Diseases* **9**, 426-431

9. Mac Kenzie, W. R., Hoxie, N. J., Proctor, M. E., Gradus, M. S., Blair, K. A., Peterson, D. E., Kazmierczak, J. J., Addiss, D. G., Fox, K. R., Rose, J. B., and et al. (1994) A massive outbreak in Milwaukee of *Cryptosporidium* infection transmitted through the public water supply. *The New England Journal of Medicine* **331**, 161-167

10. Rotz, L. D., Khan, A. S., Lillibridge, S. R., Ostroff, S. M., and Hughes, J. M. (2002) Public health assessment of potential biological terrorism agents. *Emerging Infectious Diseases* **8**, 225-230

11. Abrahamsen, M. S., Templeton, T. J., Enomoto, S., Abrahante, J. E., Zhu, G., Lancto, C. A., Deng, M., Liu, C., Widmer, G., Tzipori, S., Buck, G. A., Xu, P., Bankier, A. T., Dear, P. H., Konfortov, B. A., Spriggs, H. F., Iyer, L., Anantharaman, V., Aravind, L., and Kapur, V. (2004) Complete genome sequence of the apicomplexan, *Cryptosporidium parvum*. *Science* **304**, 441-445

12. Xu, P., Widmer, G., Wang, Y., Ozaki, L. S., Alves, J. M., Serrano, M. G., Puiu, D., Manque, P., Akiyoshi, D., Mackey, A. J., Pearson, W. R., Dear, P. H., Bankier, A. T., Peterson, D. L., Abrahamsen, M. S., Kapur, V., Tzipori, S., and Buck, G. A. (2004) The genome of *Cryptosporidium hominis*. *Nature* **431**, 1107-1112

13. Ajioka, J. W. (1997) The protozoan phylum Apicomplexa. *Methods* **13**, 79-80

14. Zhu, G., Keithly, J. S., and Philippe, H. (2000) What is the phylogenetic position of *Cryptosporidium*? *Int J Syst Evol Micr* **50**, 1673-1681

15. Fayer, R. (2008) General Biology. in *Cryptosporidium and Cryptosporidiosis* (Ronald Fayer, L. X. ed.), 2nd Ed., CRC Press, Bacon Raton, FL. pp 1-43

16. Current, W. L., and Reese, N. C. (1986) A comparison of endogenous development of three isolates of *Cryptosporidium* in suckling mice. *The Journal of Protozoology* **33**, 98-108

17. Tyzzer, E. E. (1910) An extracellular Coccidium, *Cryptosporidium Muris* (Gen. Et Sp. Nov.), of the gastric Glands of the Common Mouse. *The Journal of Medical Research* **23**, 487-510 483

18. Zhu, G., Marchewka, M. J., and Keithly, J. S. (2000) *Cryptosporidium parvum* appears to lack a plastid genome. *Microbiology* **146 (Pt 2)**, 315-321

19. Cabada, M. M., and White, A. C. (2010) Treatment of cryptosporidiosis: do we know what we think we know? *Curr Opin Infect Dis* **23**, 494-499

20. Barta, J. R., and Thompson, R. C. A. (2006) What is *Cryptosporidium*? Reappraising its biology and phylogenetic affinities. *Trends Parasitol* **22**, 463-468

21. Templeton, T. J., Enomoto, S., Chen, W. J., Huang, C. G., Lancto, C. A., Abrahamsen, M. S., and Zhu, G. (2010) A Genome-Sequence Survey for Ascogregarina taiwanensis Supports Evolutionary Affiliation but Metabolic Diversity between a *Gregarine* and *Cryptosporidium*. *Molecular Biology and Evolution* **27**, 235-248

22. Carreno, R. A., Martin, D. S., and Barta, J. R. (1999) *Cryptosporidium* is more closely related to the gregarines than to coccidia as shown by phylogenetic analysis of apicomplexan parasites inferred using small-subunit ribosomal RNA gene sequences. *Parasitol Res* **85**, 899-904

23. Lim, L., and McFadden, G. I. (2010) The evolution, metabolism and functions of the apicoplast. *Philos Trans R Soc Lond B Biol Sci* **365**, 749-763

24. Sato, S. (2011) The apicomplexan plastid and its evolution. *Cell Mol Life Sci* **68**, 1285-1296

25. Xiao, L., Fayer, R., Ryan, U., and Upton, S. J. (2004) *Cryptosporidium* taxonomy: recent advances and implications for public health. *Clinical Microbiology Reviews* **17**, 72-97

26. Hampton, J. C., and Rosario, B. (1966) The attachment of protozoan parasites to intestinalepithelial cells of the mouse. *The Journal of Parasitology* **52**, 939-949

27. Tzipori, S., Angus, K. W., Campbell, I., and Gray, E. W. (1980) *Cryptosporidium*: evidence for a single-species genus. *Infection and Immunity* **30**, 884-886

28. Tzipori, S., Smith, M., Makin, T., and Halpin, C. (1982) Enterocolitis in piglets caused by *Cryptosporidium* sp. purified from calf faeces. *Veterinary Parasitology* **11**, 121-126

29. Tzipori, S. (1983) Cryptosporidiosis in animals and humans. *Microbiological Reviews* **47**, 84-96

30. Levine, N. D. (1984) Taxonomy and review of the coccidian genus *Cryptosporidium* (protozoa, apicomplexa). *The Journal of Protozoology* **31**, 94-98

31. Fayer, R. (2010) Taxonomy and species delimitation in Cryptosporidium. *Experimental Parasitology* **124**, 90-97

32. Xiao, L. (2010) Molecular epidemiology of cryptosporidiosis: an update. *Experimental Parasitology* **124**, 80-89

33. Una Ryan, L. X. (2013) Taxonomy and molecular taxonomy. in *Cryptosporidium: Parasite and Disease* (Simone M. Caccio, G. W. ed.), Springer, New York. pp 3-41

34. Alvarez-Pellitero, P., and Sitja-Bobadilla, A. (2002) *Cryptosporidium molnari* n. sp. (Apicomplexa: Cryptosporidiidae) infecting two marine fish species, Sparus

aurata L. and Dicentrarchus labrax L. *International Journal for Parasitology* **32**, 1007-1021

35. Jirku, M., Valigurova, A., Koudela, B., Krizek, J., Modry, D., and Slapeta, J. (2008) New species of *Cryptosporidium Tyzzer*, 1907 (Apicomplexa) from amphibian host: morphology, biology and phylogeny. *Folia Parasitologica* **55**, 81-94

36. Levine, N. D. (1980) Some Corrections of Coccidian (Apicomplexa, Protozoa) Nomenclature. *Journal of Parasitology* **66**, 830-834

37. Pavlasek, I., and Ryan, U. (2008) *Cryptosporidium varanii* takes precedence over C-saurophilum. *Experimental Parasitology* **118**, 434-437

38. Slavin, D. (1955) *Cryptosporidium meleagridis* (sp. nov.). *Journal of Comparative Pathology* **65**, 262-266

39. Current, W. L., Upton, S. J., and Haynes, T. B. (1986) The life cycle of *Cryptosporidium baileyi* n. sp. (Apicomplexa, Cryptosporidiidae) infecting chickens. *The Journal of Protozoology* **33**, 289-296

40. Vetterling, J. M., Jervis, H. R., Merrill, T. G., and Sprinz, H. (1971) *Cryptosporidium wrairi* sp. n. from the guinea pig Cavia porcellus, with an emendation of the genus. *The Journal of Protozoology* **18**, 243-247

41. Iseki, M. (1979) *Cryptosporidium felis* sp. from domestic cat *Japanese Journal of Parasitology* **28**, 13-35

42. Lindsay, D. S., Upton, S. J., Owens, D. S., Morgan, U. M., Mead, J. R., and Blagburn, B. L. (2000) *Cryptosporidium andersoni* n. sp. (Apicomplexa: Cryptosporiidae) from cattle, Bos taurus. *The Journal of Eukaryotic Microbiology* **47**, 91-95

43. Fayer, R., Trout, J. M., Xiao, L., Morgan, U. M., Lai, A. A., and Dubey, J. P. (2001) *Cryptosporidium canis* n. sp. from domestic dogs. *The Journal of Parasitology* **87**, 1415-1422

44. Morgan-Ryan, U. M., Fall, A., Ward, L. A., Hijjawi, N., Sulaiman, I., Fayer, R., Thompson, R. C., Olson, M., Lal, A., and Xiao, L. (2002) *Cryptosporidium hominis* n. sp. (Apicomplexa: Cryptosporidiidae) from *Homo sapiens*. *The Journal of Eukaryotic Microbiology* **49**, 433-440

45. Ryan, U. M., Monis, P., Enemark, H. L., Sulaiman, I., Samarasinghe, B., Read, C., Buddle, R., Robertson, I., Zhou, L., Thompson, R. C., and Xiao, L. (2004)

Cryptosporidium suis n. sp. (Apicomplexa: Cryptosporidiidae) in pigs (Sus scrofa). *The Journal of Parasitology* **90**, 769-773

46. Ryan, U. M., Power, M., and Xiao, L. (2008) *Cryptosporidium fayeri* n. sp. (Apicomplexa: Cryptosporidiidae) from the Red Kangaroo (Macropus rufus). *The Journal of Eukaryotic Microbiology* **55**, 22-26

47. Power, M. L., and Ryan, U. M. (2008) A new species of *Cryptosporidium* (Apicomplexa: Cryptosporidiidae) from eastern grey kangaroos (Macropus giganteus). *The Journal of Parasitology* **94**, 1114-1117

48. Fayer, R., Santin, M., and Trout, J. M. (2008) *Cryptosporidium ryanae* n. sp. (Apicomplexa: Cryptosporidiidae) in cattle (Bos taurus). *Veterinary Parasitology* **156**, 191-198

49. Fayer, R., and Santin, M. (2009) *Cryptosporidium xiaoi* n. sp. (Apicomplexa: Cryptosporidiidae) in sheep (Ovis aries). *Veterinary Parasitology* **164**, 192-200

50. Fayer, R., Santin, M., and Macarisin, D. (2010) *Cryptosporidium ubiquitum* n. sp. in animals and humans. *Veterinary Parasitology* **172**, 23-32

51. Robinson, G., Wright, S., Elwin, K., Hadfield, S. J., Katzer, F., Bartley, P. M., Hunter, P. R., Nath, M., Innes, E. A., and Chalmers, R. M. (2010) Re-description of *Cryptosporidium cuniculus* Inman and Takeuchi, 1979 (Apicomplexa: Cryptosporidiidae): morphology, biology and phylogeny. *International Journal for Parasitology* **40**, 1539-1548

52. Ren, X., Zhao, J., Zhang, L., Ning, C., Jian, F., Wang, R., Lv, C., Wang, Q., Arrowood, M. J., and Xiao, L. (2012) *Cryptosporidium tyzzeri* n. sp. (Apicomplexa: Cryptosporidiidae) in domestic mice (Mus musculus). *Experimental Parasitology* **130**, 274-281

53. Elwin, K., Hadfield, S. J., Robinson, G., Crouch, N. D., and Chalmers, R. M. (2012) *Cryptosporidium viatorum* n. sp. (Apicomplexa: Cryptosporidiidae) among travellers returning to Great Britain from the Indian subcontinent, 2007-2011. *International Journal for Parasitology* **42**, 675-682

54. Kvac, M., Kestranova, M., Pinkova, M., Kvetonova, D., Kalinova, J., Wagnerova, P., Kotkova, M., Vitovec, J., Ditrich, O., McEvoy, J., Stenger, B., and Sak, B. (2013) *Cryptosporidium scrofarum* n. sp. (Apicomplexa: Cryptosporidiidae) in domestic pigs (Sus scrofa). *Veterinary Parasitology* **191**, 218-227

55. Carpenter, C., Fayer, R., Trout, J., and Beach, M. J. (1999) Chlorine disinfection of recreational water for Cryptosporidium parvum. *Emerging Infectious Diseases* **5**, 579-584

56. Jenkins, M. B., Eaglesham, B. S., Anthony, L. C., Kachlany, S. C., Bowman, D. D., and Ghiorse, W. C. (2010) Significance of wall structure, macromolecular composition, and surface polymers to the survival and transport of *Cryptosporidium parvum* oocysts. *Applied and Environmental Microbiology* **76**, 1926-1934

57. Fayer, R. (2008) General Biology. in *Cryptosporidium and Cryptosporidiosis* (Ronald Fayer, L. X. ed.), 2nd Ed., CRC Press, Boca Raton, FL. pp 1-42

58. Fayer, R., and Ungar, B. L. (1986) *Cryptosporidium* spp. and cryptosporidiosis. *Microbiological Reviews* **50**, 458-483

59. O'Hara, S. P., and Chen, X. M. (2011) The cell biology of *Cryptosporidium* infection. *Microbes and Infection / Institut Pasteur* **13**, 721-730

60. Vetterling, J. M., Takeuchi, A., and Madden, P. A. (1971) Ultrastructure of *Cryptosporidium wrairi* from the guinea pig. *The Journal of Protozoology* **18**, 248-260

61. Fayer, R., and Leek, R. G. (1984) The effects of reducing conditions, medium, pH, temperature, and time on in vitro excystation of Cryptosporidium. *The Journal of Protozoology* **31**, 567-569

62. Reduker, D. W., and Speer, C. A. (1985) Factors influencing excystation in *Cryptosporidium* oocysts from cattle. *The Journal of Parasitology* **71**, 112-115

63. Reduker, D. W., Speer, C. A., and Blixt, J. A. (1985) Ultrastructure of *Cryptosporidium parvum* oocysts and excysting sporozoites as revealed by high resolution scanning electron microscopy. *The Journal of Protozoology* **32**, 708-711

64. O'Hara, S. P., Yu, J. R., and Lin, J. J. (2004) A novel *Cryptosporidium parvum* antigen, CP2, preferentially associates with membranous structures. *Parasitol Res* **92**, 317-327

65. Chen, X. M., O'Hara, S. P., Huang, B. Q., Nelson, J. B., Lin, J. J., Zhu, G., Ward, H. D., and LaRusso, N. F. (2004) Apical organelle discharge by *Cryptosporidium parvum* is temperature, cytoskeleton, and intracellular calcium dependent and required for host cell invasion. *Infection and Immunity* **72**, 6806-6816

66. Chen, X. M., Keithly, J. S., Paya, C. V., and LaRusso, N. F. (2002) Cryptosporidiosis. *N Engl J Med* **346**, 1723-1731

67. Snelling, W. J., Xiao, L., Ortega-Pierres, G., Lowery, C. J., Moore, J. E., Rao, J. R., Smyth, S., Millar, B. C., Rooney, P. J., Matsuda, M., Kenny, F., Xu, J., and Dooley, J. S. (2007) Cryptosporidiosis in developing countries. *J Infect Dev Ctries* **1**, 242-256

68. Ochoa, T. J., Salazar-Lindo, E., and Cleary, T. G. (2004) Management of children with infection-associated persistent diarrhea. *Semin Pediatr Infect Dis* **15**, 229-236

69. Kotloff, K. L., Nataro, J. P., Blackwelder, W. C., Nasrin, D., Farag, T. H., Panchalingam, S., Wu, Y., Sow, S. O., Sur, D., Breiman, R. F., Faruque, A. S., Zaidi, A. K., Saha, D., Alonso, P. L., Tamboura, B., Sanogo, D., Onwuchekwa, U., Manna, B., Ramamurthy, T., Kanungo, S., Ochieng, J. B., Omore, R., Oundo, J. O., Hossain, A., Das, S. K., Ahmed, S., Qureshi, S., Quadri, F., Adegbola, R. A., Antonio, M., Hossain, M. J., Akinsola, A., Mandomando, I., Nhampossa, T., Acacio, S., Biswas, K., O'Reilly, C. E., Mintz, E. D., Berkeley, L. Y., Muhsen, K., Sommerfelt, H., Robins-Browne, R. M., and Levine, M. M. (2013) Burden and aetiology of diarrhoeal disease in infants and young children in developing countries (the Global Enteric Multicenter Study, GEMS): a prospective, case-control study. *Lancet* **382**, 209-222

70. Guerrant, D. I., Moore, S. R., Lima, A. A., Patrick, P. D., Schorling, J. B., and Guerrant, R. L. (1999) Association of early childhood diarrhea and cryptosporidiosis with impaired physical fitness and cognitive function four-seven years later in a poor urban community in northeast Brazil. *Am J Trop Med Hyg* **61**, 707-713

71. Checkley, W., Epstein, L. D., Gilman, R. H., Black, R. E., Cabrera, L., and Sterling, C. R. (1998) Effects of *Cryptosporidium parvum* infection in Peruvian children: growth faltering and subsequent catch-up growth. *Am J Epidemiol* **148**, 497-506

72. Pantenburg, B., Dann, S. M., Wang, H. C., Robinson, P., Castellanos-Gonzalez, A., Lewis, D. E., and White, A. C. (2008) Intestinal immune response to human *Cryptosporidium* sp infection. *Infection and Immunity* **76**, 23-29

73. Zhou, R., Hu, G., Liu, J., Gong, A. Y., Drescher, K. M., and Chen, X. M. (2009) NF-kappaB p65-dependent transactivation of miRNA genes following *Cryptosporidium parvum* infection stimulates epithelial cell immune responses. *PLoS Pathogens* **5**, e1000681

74. Flanigan, T., Whalen, C., Turner, J., Soave, R., Toerner, J., Havlir, D., and Kotler, D. (1992) *Cryptosporidium* infection and CD4 counts. *Annals of Internal Medicine* **116**, 840-842

75. Schmidt, W., Wahnschaffe, U., Schafer, M., Zippel, T., Arvand, M., Meyerhans, A., Riecken, E. O., and Ullrich, R. (2001) Rapid increase of mucosal CD4 T cells followed by clearance of intestinal cryptosporidiosis in an AIDS patient receiving highly active antiretroviral therapy. *Gastroenterology* **120**, 984-987

76. Heine, J., Moon, H. W., and Woodmansee, D. B. (1984) Persistent *Cryptosporidium* infection in congenitally athymic (nude) mice. *Infection and Immunity* **43**, 856-859

77. Chen, W., Harp, J. A., Harmsen, A. G., and Havell, E. A. (1993) Gamma interferon functions in resistance to *Cryptosporidium parvum* infection in severe combined immunodeficient mice. *Infection and Immunity* **61**, 3548-3551

78. McDonald, V., and Bancroft, G. J. (1994) Mechanisms of innate and acquired resistance to *Cryptosporidium parvum* infection in SCID mice. *Parasite Immunology* **16**, 315-320

79. Perryman, L. E., Mason, P. H., and Chrisp, C. E. (1994) Effect of spleen cell populations on resolution of *Cryptosporidium parvum* infection in SCID mice. *Infection and Immunity* **62**, 1474-1477

80. McDonald, V., Robinson, H. A., Kelly, J. P., and Bancroft, G. J. (1994) *Cryptosporidium muris* in adult mice: adoptive transfer of immunity and protective roles of CD4 versus CD8 cells. *Infection and Immunity* **62**, 2289-2294

81. Ungar, B. L., Kao, T. C., Burris, J. A., and Finkelman, F. D. (1991) *Cryptosporidium* infection in an adult mouse model. Independent roles for IFN-gamma and CD4+ T lymphocytes in protective immunity. *Journal of Immunology* **147**, 1014-1022

82. Aguirre, S. A., Mason, P. H., and Perryman, L. E. (1994) Susceptibility of major histocompatibility complex (MHC) class I- and MHC class II-deficient mice to *Cryptosporidium parvum* infection. *Infection and Immunity* **62**, 697-699

83. Jacyna, M. R., Parkin, J., Goldin, R., and Baron, J. H. (1990) Protracted enteric cryptosporidial infection in selective immunoglobulin A and saccharomyces opsonin deficiencies. *Gut* **31**, 714-716

84. Frost, F. J., Tollestrup, K., Craun, G. F., Fairley, C. K., Sinclair, M. I., and Kunde, T. R. (2005) Protective immunity associated with a strong serological

response to a *Cryptosporidium*-specific antigen group, in HIV-infected individuals. *The Journal of Infectious Diseases* **192**, 618-621

85. Frost, F. J., Roberts, M., Kunde, T. R., Craun, G., Tollestrup, K., Harter, L., and Muller, T. (2005) How clean must our drinking water be: the importance of protective immunity. *The Journal of Infectious Diseases* **191**, 809-814

86. Kaushik, K., Khurana, S., Wanchu, A., and Malla, N. (2009) Serum immunoglobulin G, M and A response to *Cryptosporidium parvum* in Cryptosporidium-HIV co-infected patients. *BMC Infectious Diseases* **9**, 179

87. Cozon, G., Biron, F., Jeannin, M., Cannella, D., and Revillard, J. P. (1994) Secretory IgA antibodies to *Cryptosporidium parvum* in AIDS patients with chronic cryptosporidiosis. *The Journal of Infectious Diseases* **169**, 696-699

88. Chen, W., Harp, J. A., and Harmsen, A. G. (2003) Cryptosporidium parvum infection in gene-targeted B cell-deficient mice. *The Journal of Parasitology* **89**, 391-393

89. Taghi-Kilani, R., Sekla, L., and Hayglass, K. T. (1990) The role of humoral immunity in *Cryptosporidium* spp. infection. Studies with B cell-depleted mice. *Journal of Immunology* **145**, 1571-1576

90. Hayward, A. R., Chmura, K., and Cosyns, M. (2000) Interferon-gamma is required for innate immunity to *Cryptosporidium parvum* in mice. *The Journal of Infectious Diseases* **182**, 1001-1004

91. Harp, J. A., Whitmire, W. M., and Sacco, R. (1994) In vitro proliferation and production of gamma interferon by murine CD4+ cells in response to *Cryptosporidium parvum* antigen. *The Journal of Parasitology* **80**, 67-72

92. Theodos, C. M., Sullivan, K. L., Griffiths, J. K., and Tzipori, S. (1997) Profiles of healing and nonhealing *Cryptosporidium parvum* infection in C57BL/6 mice with functional B and T lymphocytes: the extent of gamma interferon modulation determines the outcome of infection. *Infection and Immunity* **65**, 4761-4769

93. Mead, J. R., and You, X. (1998) Susceptibility differences to *Cryptosporidium parvum* infection in two strains of gamma interferon knockout mice. *The Journal of Parasitology* **84**, 1045-1048

94. Kapel, N., Benhamou, Y., Buraud, M., Magne, D., Opolon, P., and Gobert, J. G. (1996) Kinetics of mucosal ileal gamma-interferon response during cryptosporidiosis in immunocompetent neonatal mice. *Parasitol Res* **82**, 664-667

95. Fayer, R., Gasbarre, L., Pasquali, P., Canals, A., Almeria, S., and Zarlenga, D. (1998) *Cryptosporidium parvum* infection in bovine neonates: dynamic clinical, parasitic and immunologic patterns. *International Journal for Parasitology* **28**, 49-56

96. Wyatt, C. R., Brackett, E. J., and Savidge, J. (2001) Evidence for the emergence of a type-1-like immune response in intestinal mucosa of calves recovering from cryptosporidiosis. *The Journal of Parasitology* **87**, 90-95

97. White, A. C., Robinson, P., Okhuysen, P. C., Lewis, D. E., Shahab, I., Lahoti, S., DuPont, H. L., and Chappell, C. L. (2000) Interferon-gamma expression in jejunal biopsies in experimental human cryptosporidiosis correlates with prior sensitization and control of oocyst excretion. *The Journal of Infectious Diseases* **181**, 701-709

98. Trinchieri, G. (2003) Interleukin-12 and the regulation of innate resistance and adaptive immunity. *Nature Reviews Immunology* **3**, 133-146

99. Urban, J. F., Jr., Fayer, R., Chen, S. J., Gause, W. C., Gately, M. K., and Finkelman, F. D. (1996) IL-12 protects immunocompetent and immunodeficient neonatal mice against infection with *Cryptosporidium parvum*. *Journal of Immunology* **156**, 263-268

100. McDonald, S. A., O'Grady, J. E., Bajaj-Elliott, M., Notley, C. A., Alexander, J., Brombacher, F., and McDonald, V. (2004) Protection against the early acute phase of *Cryptosporidium parvum* infection conferred by interleukin-4-induced expression of T helper 1 cytokines. *The Journal of Infectious Diseases* **190**, 1019-1025

101. Campbell, L. D., Stewart, J. N., and Mead, J. R. (2002) Susceptibility to *Cryptosporidium parvum* infections in cytokine- and chemokine-receptor knockout mice. *The Journal of Parasitology* **88**, 1014-1016

102. Tzipori, S., and Ward, H. (2002) Cryptosporidiosis: biology, pathogenesis and disease. *Microbes Infect* **4**, 1047-1058

103. Miao, Y. M., Awad-El-Kariem, F. M., Franzen, C., Ellis, D. S., Muller, A., Counihan, H. M., Hayes, P. J., and Gazzard, B. G. (2000) Eradication of cryptosporidia and microsporidia following successful antiretroviral therapy. *Journal of Acquired Immune Deficiency Syndromes* **25**, 124-129

104. Babiker, A., Darbyshire, J., Pezzotti, P., Porter, K., Rezza, G., Walker, S. A., Beral, V., Coutinho, R., Del Amo, J., Gill, N., Lee, C., Meyer, L., Tyrer, F., Dabis, F., Thiebaut, R., Lawson-Aye, S., Boufassa, F., Hamouda, O., Fischer, K., Pezzotti, P., Rezza, G., Touloumi, G., Hatzakis, A., Karafoulidou, A., Katsarou,

O., Brettle, R., del Romero, J., Prins, M., van Benthem, B., Kirk, O., Pederson, C., Hernandez Aguado, I., Perez-Hoyos, S., Eskild, A., Bruun, J. N., Sannes, M., Sabin, C., Lee, C., Johnson, A. M., Phillips, A. N., Francioli, P., Vanhems, P., Egger, M., Rickenbach, M., Cooper, D., Kaldor, J., Ashton, L., Vizzard, J., Muga, R., Day, N. E., De Angelis, D., and Collaboration, C. (2002) Changes over calendar time in the risk of specific first AIDS-defining events following HIV seroconversion, adjusting for competing risks. *International Journal of Epidemiology* **31**, 951-958

105. Mele, R., Gomez Morales, M. A., Tosini, F., and Pozio, E. (2003) Indinavir reduces *Cryptosporidium parvum* infection in both in vitro and in vivo models. *International Journal for Parasitology* **33**, 757-764

106. Hommer, V., Eichholz, J., and Petry, F. (2003) Effect of antiretroviral protease inhibitors alone, and in combination with paromomycin, on the excystation, invasion and in vitro development of *Cryptosporidium parvum*. *The Journal of Antimicrobial Chemotherapy* **52**, 359-364

107. Alfonso, Y., and Monzote, L. (2011) HIV Protease Inhibitors: Effect on the Opportunistic Protozoan Parasites. *The Open Medicinal Chemistry Journal* **5**, 40-50

108. Clezy, K., Gold, J., Blaze, J., and Jones, P. (1991) Paromomycin for the treatment of cryptosporidial diarrhoea in AIDS patients. *Aids* **5**, 1146-1147

109. Fichtenbaum, C. J., Ritchie, D. J., and Powderly, W. G. (1993) Use of paromomycin for treatment of cryptosporidiosis in patients with AIDS. *Clinical Infectious Diseases : an Official Publication of the Infectious Diseases Society of America* **16**, 298-300

110. Wallace, M. R., Nguyen, M. T., and Newton, J. A., Jr. (1993) Use of paromomycin for the treatment of cryptosporidiosis in patients with AIDS. *Clinical Infectious Diseases : an Official Publication of the Infectious Diseases Society of America* **17**, 1070-1071

111. White, A. C., Jr., Chappell, C. L., Hayat, C. S., Kimball, K. T., Flanigan, T. P., and Goodgame, R. W. (1994) Paromomycin for cryptosporidiosis in AIDS: a prospective, double-blind trial. *The Journal of Infectious Diseases* **170**, 419-424

112. Hewitt, R. G., Yiannoutsos, C. T., Higgs, E. S., Carey, J. T., Geiseler, P. J., Soave, R., Rosenberg, R., Vazquez, G. J., Wheat, L. J., Fass, R. J., Antoninievic, Z., Walawander, A. L., Flanigan, T. P., Bender, J. F., and Grp, A. C. T. (2000) Paromomycin: No more effective than placebo for treatment of cryptosporidiosis in patients with advanced human immunodeficiency virus infection. *Clinical Infectious Diseases* **31**, 1084-1092

113. Kaplan, J. E., Benson, C., Holmes, K. K., Brooks, J. T., Pau, A., Masur, H., Centers for Disease, C., Prevention, National Institutes of, H., and America, H. I. V. M. A. o. t. I. D. S. o. (2009) Guidelines for prevention and treatment of opportunistic infections in HIV-infected adults and adolescents: recommendations from CDC, the National Institutes of Health, and the HIV Medicine Association of the Infectious Diseases Society of America. *MMWR. Recommendations and Reports : Morbidity and Mortality Weekly Report. Recommendations and Reports / Centers for Disease Control* **58**, 1-207; quiz CE201-204

114. Rossignol, J. F., Ayoub, A., and Ayers, M. S. (2001) Treatment of diarrhea caused by *Cryptosporidium parvum*: a prospective randomized, double-blind, placebo-controlled study of Nitazoxanide. *The Journal of Infectious Diseases* **184**, 103-106

115. Rossignol, J. F., Hidalgo, H., Feregrino, M., Higuera, F., Gomez, W. H., Romero, J. L., Padierna, J., Geyne, A., and Ayers, M. S. (1998) A double-'blind' placebo-controlled study of nitazoxanide in the treatment of cryptosporidial diarrhoea in AIDS patients in Mexico. *Transactions of the Royal Society of Tropical Medicine and Hygiene* **92**, 663-666

116. Amadi, B., Mwiya, M., Musuku, J., Watuka, A., Sianongo, S., Ayoub, A., and Kelly, P. (2002) Effect of nitazoxanide on morbidity and mortality in Zambian children with cryptosporidiosis: a randomised controlled trial. *Lancet* **360**, 1375-1380

117. Amadi, B., Mwiya, M., Sianongo, S., Payne, L., Watuka, A., Katubulushi, M., and Kelly, P. (2009) High dose prolonged treatment with nitazoxanide is not effective for cryptosporidiosis in HIV positive Zambian children: a randomised controlled trial. *BMC Infectious Diseases* **9**, 195

118. World-Health-Organization. (2013) Global update on HIV treatment 2013: results, imparct and opportunities. Publications of the World Health Organization, 1211 Geneva 27, Switzerland

119. Amadi, B., Kelly, P., Mwiya, M., Mulwazi, E., Sianongo, S., Changwe, F., Thomson, M., Hachungula, J., Watuka, A., Walker-Smith, J., and Chintu, C. (2001) Intestinal and systemic infection, HIV, and mortality in Zambian children with persistent diarrhea and malnutrition. *Journal of Pediatric Gastroenterology and Nutrition* **32**, 550-554

120. Guerrant, D. I., Moore, S. R., Lima, A. A., Patrick, P. D., Schorling, J. B., and Guerrant, R. L. (1999) Association of early childhood diarrhea and cryptosporidiosis with impaired physical fitness and cognitive function four-

seven years later in a poor urban community in northeast Brazil. *The American Journal of Tropical Medicine and Hygiene* **61**, 707-713

121. Tumwine, J. K., Kekitiinwa, A., Nabukeera, N., Akiyoshi, D. E., Rich, S. M., Widmer, G., Feng, X., and Tzipori, S. (2003) *Cryptosporidium parvum* in children with diarrhea in Mulago Hospital, Kampala, Uganda. *The American Journal of Tropical Medicine and Hygiene* **68**, 710-715

122. Artz, J. D., Dunford, J. E., Arrowood, M. J., Dong, A., Chruszcz, M., Kavanagh, K. L., Minor, W., Russell, R. G., Ebetino, F. H., Oppermann, U., and Hui, R. (2008) Targeting a uniquely nonspecific prenyl synthase with bisphosphonates to combat cryptosporidiosis. *Chemistry & Biology* **15**, 1296-1306

123. Popov, V. M., Chan, D. C., Fillingham, Y. A., Atom Yee, W., Wright, D. L., and Anderson, A. C. (2006) Analysis of complexes of inhibitors with *Cryptosporidium hominis* DHFR leads to a new trimethoprim derivative. *Bioorganic & Medicinal Chemistry Letters* **16**, 4366-4370

124. Sun, X. E., Sharling, L., Muthalagi, M., Mudeppa, D. G., Pankiewicz, K. W., Felczak, K., Rathod, P. K., Mead, J., Striepen, B., and Hedstrom, L. (2010) Prodrug activation by *Cryptosporidium* thymidine kinase. *The Journal of Biological Chemistry* **285**, 15916-15922

125. Sharling, L., Liu, X., Gollapalli, D. R., Maurya, S. K., Hedstrom, L., and Striepen, B. (2010) A screening pipeline for antiparasitic agents targeting *Cryptosporidium* inosine monophosphate dehydrogenase. *PLoS Neglected Tropical Diseases* **4**, e794

126. Zhu, G. (2004) Current progress in the fatty acid metabolism in *Cryptosporidium parvum*. *The Journal of Eukaryotic Microbiology* **51**, 381-388

127. Zeng, B., Cai, X., and Zhu, G. (2006) Functional characterization of a fatty acyl-CoA-binding protein (ACBP) from the apicomplexan *Cryptosporidium parvum*. *Microbiology* **152**, 2355-2363

128. Fritzler, J. M., Millership, J. J., and Zhu, G. (2007) *Cryptosporidium parvum* long-chain fatty acid elongase. *Eukaryot Cell* **6**, 2018-2028

129. Zhu, G., Shi, X., and Cai, X. (2010) The reductase domain in a Type I fatty acid synthase from the apicomplexan *Cryptosporidium parvum*: restricted substrate preference towards very long chain fatty acyl thioesters. *BMC Biochemistry* **11**, 46

130. Zhu, G., Marchewka, M. J., Woods, K. M., Upton, S. J., and Keithly, J. S. (2000) Molecular analysis of a Type I fatty acid synthase in *Cryptosporidium parvum*. *Molecular and Biochemical Parasitology* **105**, 253-260

131. Zhu, G., Li, Y., Cai, X., Millership, J. J., Marchewka, M. J., and Keithly, J. S. (2004) Expression and functional characterization of a giant Type I fatty acid synthase (CpFAS1) gene from *Cryptosporidium parvum*. *Molecular and Biochemical Parasitology* **134**, 127-135

132. Shanmugasundram, A., Gonzalez-Galarza, F. F., Wastling, J. M., Vasieva, O., and Jones, A. R. (2013) Library of Apicomplexan Metabolic Pathways: a manually curated database for metabolic pathways of apicomplexan parasites. *Nucleic Acids Research* **41**, D706-713

133. Fritzler, J. M., Millership, J. J., and Zhu, G. (2007) *Cryptosporidium parvum* long-chain fatty acid elongase. *Eukaryotic Cell* **6**, 2018-2028

134. Andersson, C. S., Lundgren, C. A., Magnusdottir, A., Ge, C., Wieslander, A., Martinez Molina, D., and Hogbom, M. (2012) The *Mycobacterium tuberculosis* very-long-chain fatty acyl-CoA synthetase: structural basis for housing lipid substrates longer than the enzyme. *Structure* **20**, 1062-1070

135. Fujino, T., Kang, M. J., Suzuki, H., Iijima, H., and Yamamoto, T. (1996) Molecular characterization and expression of rat acyl-CoA synthetase 3. *J Biol Chem* **271**, 16748-16752

136. Berthiaume, L., Deichaite, I., Peseckis, S., and Resh, M. D. (1994) Regulation of enzymatic activity by active site fatty acylation. A new role for long chain fatty acid acylation of proteins. *J Biol Chem* **269**, 6498-6505

137. Marin, E. P., Derakhshan, B., Lam, T. T., Davalos, A., and Sessa, W. C. (2012) Endothelial cell palmitoylproteomic identifies novel lipid-modified targets and potential substrates for protein acyl transferases. *Circ Res* **110**, 1336-1344

138. Tomoda, H., Igarashi, K., Cyong, J. C., and Omura, S. (1991) Evidence for an essential role of long chain acyl-CoA synthetase in animal cell proliferation. Inhibition of long chain acyl-CoA synthetase by triacsins caused inhibition of Raji cell proliferation. *J Biol Chem* **266**, 4214-4219

139. Glick, B. S., and Rothman, J. E. (1987) Possible Role for Fatty Acyl-Coenzyme-a in Intracellular Protein-Transport. *Nature* **326**, 309-312

140. Korchak, H. M., Kane, L. H., Rossi, M. W., and Corkey, B. E. (1994) Long chain acyl coenzyme A and signaling in neutrophils. An inhibitor of acyl coenzyme A

synthetase, triacsin C, inhibits superoxide anion generation and degranulation by human neutrophils. *J Biol Chem* **269**, 30281-30287

141. Faergeman, N. J., and Knudsen, J. (1997) Role of long-chain fatty acyl-CoA esters in the regulation of metabolism and in cell signalling. *Biochem J* **323 (Pt 1)**, 1-12

142. Weimar, J. D., DiRusso, C. C., Delio, R., and Black, P. N. (2002) Functional role of fatty acyl-coenzyme A synthetase in the transmembrane movement and activation of exogenous long-chain fatty acids. Amino acid residues within the ATP/AMP signature motif of *Escherichia coli* FadD are required for enzyme activity and fatty acid transport. *J Biol Chem* **277**, 29369-29376

143. Zou, Z., Tong, F., Faergeman, N. J., Borsting, C., Black, P. N., and DiRusso, C. C. (2003) Vectorial acylation in *Saccharomyces cerevisiae*. Fat1p and fatty acyl-CoA synthetase are interacting components of a fatty acid import complex. *J Biol Chem* **278**, 16414-16422

144. Black, P. N., Zhang, Q., Weimar, J. D., and DiRusso, C. C. (1997) Mutational analysis of a fatty acyl-coenzyme A synthetase signature motif identifies seven amino acid residues that modulate fatty acid substrate specificity. *J Biol Chem* **272**, 4896-4903

145. DiRusso, C. C., Black, P. N., and Weimar, J. D. (1999) Molecular inroads into the regulation and metabolism of fatty acids, lessons from bacteria. *Prog Lipid Res* **38**, 129-197

146. Faergeman, N. J., Black, P. N., Zhao, X. D., Knudsen, J., and DiRusso, C. C. (2001) The acyl-CoA synthetases encoded within FAA1 and FAA4 in *Saccharomyces cerevisiae* function as components of the fatty acid transport system linking import, activation, and intracellular utilization. *Journal of Biological Chemistry* **276**, 37051-37059

147. Zhu, G., Li, Y., Cai, X., Millership, J. J., Marchewka, M. J., and Keithly, J. S. (2004) Expression and functional characterization of a giant Type I fatty acid synthase (CpFAS1) gene from *Cryptosporidium parvum*. *Mol Biochem Parasitol* **134**, 127-135

148. Matesanz, F., Tellez, M. M., and Alcina, A. (2003) The *Plasmodium falciparum* fatty acyl-CoA synthetase family (PfACS) and differential stage-specific expression in infected erythrocytes. *Mol Biochem Parasitol* **126**, 109-112

149. Arrowood, M. J., and Sterling, C. R. (1987) Isolation of Cryptosporidium Oocysts and Sporozoites Using Discontinuous Sucrose and Isopycnic Percoll Gradients. *The Journal of Parasitology* **73**, 314-319

150. Zhang, H., Guo, F., and Zhu, G. (2012) Involvement of Host Cell Integrin alpha2 in *Cryptosporidium parvum* Infection. *Infect Immun* **80**, 1753-1758

151. Robertson, L. J., Campbell, A. T., and Smith, H. V. (1993) In vitro excystation of *Cryptosporidium parvum*. *Parasitology* **106 (Pt 1)**, 13-19

152. Cai, X., Woods, K. M., Upton, S. J., and Zhu, G. (2005) Application of quantitative real-time reverse transcription-PCR in assessing drug efficacy against the intracellular pathogen *Cryptosporidium parvum* in vitro. *Antimicrob Agents Chemother* **49**, 4437-4442

153. Kurien, B. T. (2009) Affinity purification of autoantibodies from an antigen strip excised from a nitrocellulose protein blot. *Methods Mol Biol* **536**, 201-211

154. Bernson, V. S. M. (1976) Acetyl-Coa Hydrolase - Activity, Regulation and Physiological Significance of Enzyme in Brown Adipose-Tissue from Hamster. *European Journal of Biochemistry* **67**, 403-410

155. Zhuravleva, E., Gut, H., Hynx, D., Marcellin, D., Bleck, C. K., Genoud, C., Cron, P., Keusch, J. J., Dummler, B., Esposti, M. D., and Hemmings, B. A. (2012) Acyl coenzyme A thioesterase Them5/Acot15 is involved in cardiolipin remodeling and fatty liver development. *Mol Cell Biol* **32**, 2685-2697

156. Arrowood, M. J., Hurd, M. R., and Mead, J. R. (1995) A new method for evaluating experimental cryptosporidial parasite loads using immunofluorescent flow cytometry. *The Journal of Parasitology* **81**, 404-409

157. Arrowood, M. J., and Donaldson, K. (1996) Improved purification methods for calf-derived *Cryptosporidium parvum* oocysts using discontinuous sucrose and cesium chloride gradients. *J Eukaryot Microbiol* **43**, 89S

158. Soupene, E., and Kuypers, F. A. (2008) Mammalian long-chain acyl-CoA synthetases. *Exp Biol Med (Maywood)* **233**, 507-521

159. Schnurr, J., Shockey, J., and Browse, J. (2004) The acyl-CoA synthetase encoded by LACS2 is essential for normal cuticle development in *Arabidopsis*. *Plant Cell* **16**, 629-642

160. Melton, E. M., Cerny, R. L., Watkins, P. A., DiRusso, C. C., and Black, P. N. (2011) Human fatty acid transport protein 2a/very long chain acyl-CoA synthetase 1 (FATP2a/Acsvl1) has a preference in mediating the channeling of exogenous n-3 fatty acids into phosphatidylinositol. *J Biol Chem* **286**, 30670-30679

161. Perkins, M. E., Riojas, Y. A., Wu, T. W., and Le Blancq, S. M. (1999) CpABC, a *Cryptosporidium parvum* ATP-binding cassette protein at the host-parasite boundary in intracellular stages. *Proceedings of the National Academy of Sciences of the United States of America* **96**, 5734-5739

162. Fritzler, J. M., and Zhu, G. (2007) Functional characterization of the acyl-[acyl carrier protein] ligase in the *Cryptosporidium parvum* giant polyketide synthase. *Int J Parasitol* **37**, 307-316

163. Matesanz, F., Duran-Chica, I., and Alcina, A. (1999) The cloning and expression of Pfacs1, a *Plasmodium falciparum* fatty acyl coenzyme A synthetase-1 targeted to the host erythrocyte cytoplasm. *J Mol Biol* **291**, 59-70

164. Ichihara, K., and Shibasaki, Y. (1991) An enzyme-coupled assay for acyl-CoA synthetase. *J Lipid Res* **32**, 1709-1712

165. Yoshida, K., Okamoto, M., Umehara, K., Iwami, M., Kohsaka, M., Aoki, H., and Imanaka, H. (1982) Studies on new vasodilators, WS-1228 A and B. I. Discovery, taxonomy, isolation and characterization. *J Antibiot (Tokyo)* **35**, 151-156

166. Tanaka, H., Yoshida, K., Itoh, Y., and Imanaka, H. (1982) Studies on new vasodilators, WS-1228 A and B. II. Structure and synthesis. *J Antibiot (Tokyo)* **35**, 157-163

167. Tomoda, H., Igarashi, K., and Omura, S. (1987) Inhibition of acyl-CoA synthetase by triacsins. *Biochim Biophys Acta* **921**, 595-598

168. Omura, S., Tomoda, H., Xu, Q. M., Takahashi, Y., and Iwai, Y. (1986) Triacsins, new inhibitors of acyl-CoA synthetase produced by Streptomyces sp. *J Antibiot (Tokyo)* **39**, 1211-1218

169. Hartman, E. J., Omura, S., and Laposata, M. (1989) Triacsin C: a differential inhibitor of arachidonoyl-CoA synthetase and nonspecific long chain acyl-CoA synthetase. *Prostaglandins* **37**, 655-671

170. Vessey, D. A., Kelley, M., and Warren, R. S. (2004) Characterization of triacsin C inhibition of short-, medium-, and long-chain fatty acid: CoA ligases of human liver. *J Biochem Mol Toxicol* **18**, 100-106

171. Kim, J. H., Lewin, T. M., and Coleman, R. A. (2001) Expression and characterization of recombinant rat Acyl-CoA synthetases 1, 4, and 5. Selective inhibition by triacsin C and thiazolidinediones. *J Biol Chem* **276**, 24667-24673

172. Van Horn, C. G., Caviglia, J. M., Li, L. O., Wang, S., Granger, D. A., and Coleman, R. A. (2005) Characterization of recombinant long-chain rat acyl-CoA synthetase isoforms 3 and 6: identification of a novel variant of isoform 6. *Biochemistry* **44**, 1635-1642

173. Cheng, Y., and Prusoff, W. H. (1973) Relationship between the inhibition constant (K1) and the concentration of inhibitor which causes 50 per cent inhibition (I50) of an enzymatic reaction. *Biochem Pharmacol* **22**, 3099-3108

174. Stockdale, H. D., Spencer, J. A., and Blagburn, B. L. (2007) *Prophylaxis and Chemotherapy*, 2nd ed., CRC Press, Boca Raton

175. Mashima, T., Sato, S., Okabe, S., Miyata, S., Matsuura, M., Sugimoto, Y., Tsuruo, T., and Seimiya, H. (2009) Acyl-CoA synthetase as a cancer survival factor: its inhibition enhances the efficacy of etoposide. *Cancer Sci* **100**, 1556-1562

176. Matsuda, D., Namatame, I., Ohshiro, T., Ishibashi, S., Omura, S., and Tomoda, H. (2008) Anti-atherosclerotic activity of triacsin C, an acyl-CoA synthetase inhibitor. *J Antibiot* **61**, 318-321

177. Beaumelle, B. D., and Vial, H. J. (1988) Acyl-CoA synthetase activity in Plasmodium knowlesi-infected erythrocytes displays peculiar substrate specificities. *Biochim Biophys Acta* **958**, 1-9

178. Camero, L., Shulaw, W. P., and Xiao, L. (2003) Characterization of a *Cryptosporidium parvum* gene encoding a protein with homology to long chain fatty acid synthetase. *J Eukaryot Microbiol* **50 Suppl**, 534-538

179. Black, P. N., Zhang, Q., Weimar, J. D., and DiRusso, C. C. (1997) Mutational analysis of a fatty acyl-coenzyme A synthetase signature motif identifies seven amino acid residues that modulate fatty acid substrate specificity. *Journal of Biological Chemistry* **272**, 4896-4903

180. Theodos, C. M., Griffiths, J. K., D'Onfro, J., Fairfield, A., and Tzipori, S. (1998) Efficacy of nitazoxanide against *Cryptosporidium parvum* in cell culture and in animal models. *Antimicrob Agents Chemother* **42**, 1959-1965

181. Fujimoto, Y., Onoduka, J., Homma, K. J., Yamaguchi, S., Mori, M., Higashi, Y., Makita, M., Kinoshita, T., Noda, J., Itabe, H., and Takanoa, T. (2006) Long-chain fatty acids induce lipid droplet formation in a cultured human hepatocyte in a manner dependent of Acyl-CoA synthetase. *Biol Pharm Bull* **29**, 2174-2180

182. Igal, R. A., Wang, P., and Coleman, R. A. (1997) Triacsin C blocks de novo synthesis of glycerolipids and cholesterol esters but not recycling of fatty acid

into phospholipid: evidence for functionally separate pools of acyl-CoA. *Biochem J* **324 (Pt 2)**, 529-534

183. Xie, Y. L., Pan, Y. E., Chang, C. J., Tang, P. C., Huang, Y. F., Walzem, R. L., and Chen, S. E. (2012) Palmitic acid in chicken granulosa cell death-lipotoxic mechanisms mediate reproductive inefficacy of broiler breeder hens. *Theriogenology* **78**, 1917-1928

184. Matsuda, D., Namatame, I., Ohshiro, T., Ishibashi, S., Omura, S., and Tomoda, H. (2008) Anti-atherosclerotic activity of triacsin C, an acyl-CoA synthetase inhibitor. *J Antibiot (Tokyo)* **61**, 318-321

185. Chen, X. M., Keithly, J. S., Paya, C. V., and LaRusso, N. F. (2002) Cryptosporidiosis. *The New England Journal of Medicine* **346**, 1723-1731